https://doi.org/10.5194/egusphere-2025-1106
Preprint. Discussion started: 14 March 2025

Palaeoclimate synthesis of the central Mediterranean area from pollen data

Léa d'Oliveira[1], Sébastien Joannin[1], Guillemette Ménot[2], Nathalie Combourieu-Nebout[3], Lucas Dugerdil[1,2], Marion Blache[1,4], Mary Robles[5], Assunta Florenzano[6], Alessia Masi[7], Anna Maria Mercuri[6], Laura Sadori[7], Marie Balasse[8], and Odile Peyron[1]

[1]Université de Montpellier, CNRS, IRD, EPHE, UMR 5554 ISEM, 34090, Montpellier, France
[2]Univ. Lyon, ENS de Lyon, Université Lyon 1, CNRS, UMR 5276 LGL-TPE, 69364, Lyon, France
[3]Muséum national d'Histoire naturelle, CNRS, MNHN, UMR 7194 HNPH, 75116, Paris, France
[4]Université du Québec en Abitibi-Témiscamingue, IRF, Québec, Canada
[5]Université Aix Marseille, CNRS, IRD, INRAE, Collège de France, UMR 7330 CEREGE, 13545, Aix-en-Provence, France
[6]University of Modena and Reggio Emilia, LPP, 41121, Modena, Italy
[7]Sapienza University of Rome, DBA, 00185, Rome, Italy
[8]Muséum national d'Histoire naturelle, CNRS, MNHN, UMR 7209 BioArch, 75116, Paris, France

Correspondence: Léa d'Oliveira (lea.d-oliveira@umontpellier.fr)

Abstract. Mediterranean climate is characterised by a strong seasonality, critical for the ecosystems and societies in the region and is susceptible to climate change. The timing of when the Mediterranean climate developed over the past few thousand years remains a complex and unresolved question. Most studies document a part of the Mediterranean area or are based on a single (and frequently different) climate reconstruction method which can lead to non-negligible biases when considering climate changes on a Mediterranean scale. Several climate summaries based on pollen data have recently been produced on a European scale. However, none of them has focused exclusively on the Mediterranean area, except two recent syntheses documenting the eastern and western parts of the Mediterranean basin. We aimed to document the climate changes of the central Mediterranean during the Holocene, the trends and the different patterns. A robust methodology has been applied to 38 pollen records spreading across the south of France and Italy. Four climate reconstruction methods based on different mathematical and ecological concepts have been tested (MAT, WA-PLS, BRT and RF) and the selection of the best modern calibration dataset has also been investigated to produce the most reliable results. Particular attention has been paid to the seasonal nature of climatic parameters (winter and summer temperatures and precipitations). A model-data comparison has been made using transient model simulation TraCE-21ka in an attempt to gain a better understanding of the climate mechanisms and their forcing. Our palaeoclimate reconstruction shows that during the mid Holocene, summer temperatures were colder in the southern part of the central Mediterranean region albeit associated with positive anomalies, which is in accordance with the summer temperature reconstructions of the Iberian peninsula and eastern Mediterranean for the mid Holocene. In northern parts of the central Mediterranean region, and particularly in high elevation (> 1000 m), a Holocene thermal maximum is present, contrasting with the cold summer temperature anomalies previously reconstructed with pollen data for the Mediterranean region. Holocene summer conditions were characterised by specific spatio-temporal patterns, i.e., a west-east differentiation in southern France and a north-south one in Italy, for both temperature and precipitation. Holocene winter conditions showed

https://doi.org/10.5194/egusphere-2025-1106
Preprint. Discussion started: 14 March 2025

a more homogeneous spatio-temporal pattern, i.e., general humidification and warming through the Holocene for Italy and southern France. A data–model simulation comparison show a mostly coherent signal in winter but an incoherent one in summer. Those discrepancies between model simulations and pollen-based reconstructions suggest that during the Holocene, the northern Mediterranean climate was already subject to a marked spatio-temporal variability, particularly in summer, that cannot only be explained by changes in orbital configuration and atmospheric greenhouse gas evolution. Finally, our result highlighted the onset of the "Mediterraneanization" of the central Mediterranean region, characterised by wet winters and dry summers, after 8,000 years BP. The "Mediterraneanization" process seems to have had a greater impact on the southern regions than on the northern regions.

1 Introduction

Placing recent global warming in the context of natural climate variability requires a long-term perspective. Climate changes during the Holocene (the last 11,700 years BP) have been extensively documented by various palaeoclimate proxy records, revealing complex and heterogeneous spatio-temporal patterns in Europe (e.g., Cheddadi et al., 1997; Davis et al., 2003; Magny et al., 2003; Bartlein et al., 2011; Kaufman et al., 2020b; Herzschuh et al., 2023a). These climate patterns may be linked to regional characteristics (e.g., latitude or elevation) or seasonal variables (e.g., summer or winter) (Mauri et al., 2015; Cartapanis et al., 2022; Erb et al., 2022) which can in turn impact how well the pattern is recorded. This effect is well illustrated by the temperature warming between 10,000 and 6,000 years BP also called mid Holocene thermal maximum (HTM), well evidenced in northern Europe (Renssen et al., 2012; Liu et al., 2014) but poorly recorded in southern Europe (Kaufman et al., 2020b; Marriner et al., 2022).

In the Mediterranean area, terrestrial proxies suggest conditions similar to or cooler than those observed today (Cheddadi et al., 1997; Davis et al., 2003; Herzschuh et al., 2023a). However, since the last decades, atmospheric climate models often fail to simulate the mid Holocene Mediterranean cooling, producing significant warming both in northern and southern Europe (Liu et al., 2014; Mauri et al., 2014; Erb et al., 2022). Recent model studies are in better agreement with the data as they integrate the soil-atmosphere interactions in their model simulations (Russo and Cubasch, 2016; Russo et al., 2022) but the underlying climate mechanisms are not yet fully understood. This is still a key question, as most data or model studies focus on the European region or the world as a whole (Cheddadi et al., 1997; Davis et al., 2003; Mauri et al., 2015; Marsicek et al., 2018; Kaufman et al., 2020b; Cartapanis et al., 2022; Erb et al., 2022; Herzschuh et al., 2023a), but very little on the Mediterranean region, which is in the end very little studied on a broad scale (Magny et al., 2012; Peyron et al., 2017; Finné et al., 2019; Marriner et al., 2022).

The Mediterranean region is located in a complex transitional zone, influenced by both the tropical circulation cells and the mid-latitude westerlies and cyclogenesis, which exposes the basin to a relatively large spectrum of climatic influences from the arid zone of the subtropical high to the humid north-westerly air flows (Margaritelli et al., 2020). In summer, the Mediterranean region is under the influence of subtropical climate, which is strongly linked to the Inter-Tropical Convergence Zone (ITCZ) position. In winter however, the subtropical high-pressure belt is shifted southward and the Mediterranean region is mainly

https://doi.org/10.5194/egusphere-2025-1106
Preprint. Discussion started: 14 March 2025

linked to the westerly system bringing an eastward important water influx (Giraudi et al., 2011; Goudeau et al., 2015). This results in a pronounced rainfall seasonality that is critical for ecosystems and societies in the Mediterranean region today and in the past (Cramer et al., 2018) and points out the need for seasonal scale reconstructions over annual ones (Goudeau et al., 2015).

Few studies have attempted to better understand the climate changes at a regional scale in the Mediterranean region during the Holocene (Jalut et al., 2000; Magny et al., 2013; Peyron et al., 2017; Finné et al., 2019). Documenting these climate changes with precision is complex, as the reconstructed climate patterns may be linked to regional characteristics (e.g., longitude, latitude, and elevation), seasonal variables (e.g., summer or winter), or specific to the proxy used (pollen, chironomids, marine proxies, molecular biomarkers). Specific temperature and precipitation patterns have been suggested as a west–east (Dormoy et al., 2009; Liu et al., 2023) as well as a north–south gradient within the Mediterranean basin (Magny et al., 2012, 2013; Peyron et al., 2017). These studies concluded that, over the past 10,000 years, the Mediterranean basin has not been defined by a singular climate trajectory, making our understanding of the spatio-temporal variability of the Mediterranean climate still incomplete. Similarly, the intensity of seasonal variations, e.g., the differences between summer and winter conditions, and their evolution through time also seem to vary greatly from one region to another during the Holocene (Roberts et al., 2011; Peyron et al., 2017).

Climatic reconstructions can be highly dependent on the proxies used (Samartin et al., 2017; Kaufman et al., 2020a; Cartapanis et al., 2022). The reconstructions based on chironomids data disagree with the pollen-based ones (Samartin et al., 2017; Cartapanis et al., 2022). To reconstruct past climate changes in the Mediterranean area, most studies are based on a multi-proxy approach focusing on either terrestrial and marine records (lake levels, fluvial activity, pollen records, Jalut, 2000; Roberts et al., 2011; Finné et al., 2019; Cartapanis et al., 2022; Marriner et al., 2022) as well as only pollen-based approaches (Davis et al., 2003; Mauri et al., 2015; Peyron et al., 2017; Cruz-Silva et al., 2023; Liu et al., 2023). Pollen is the most widely used proxy for palaeoclimate studies because of the excellent spatial coverage it provides, but also because the relationship between vegetation and climate is well known, giving good robustness to palaeoclimate reconstructions based on pollen. However, most of these studies use different climate reconstruction methods (transfer functions), different pollen datasets, and different climatic (e.g., precipitation, temperature) or bioclimatic (e.g., growing degree day, evapotranspiration) parameters. Such differences may influence the reliability of the results (Chevalier et al., 2020).

Recently, two regional syntheses based on high-quality pollen data have been performed to reconstruct the climate changes of the western Mediterranean region, i.e., the Iberian Peninsula (brown dots on Fig. 1, Liu et al., 2023), and of the eastern Mediterranean (blue dots on Fig. 1, Cruz-Silva et al., 2023). They highlighted complex spatio-temporal changes in the two Mediterranean key regions and, as a result, pointed out our lack of understanding of the intermediate sub-regions of the north-central Mediterranean, encompassing Southern France and Italy.

In this frame, our study aims to reconstruct the spatio-temporal climate variability of this central region to better understand and discuss the climate changes at the scale of the Mediterranean area. Our questions are : (1) what were the climate conditions during the mid Holocene: should we reconstruct colder than today's conditions as in previous pollen-based studies? Is the HTM recorded in the Mediterranean area during the early to mid Holocene as shown by marine proxies? (2) Is there a

https://doi.org/10.5194/egusphere-2025-1106
Preprint. Discussion started: 14 March 2025

north–south climate pattern across the Italian peninsula and adjacent regions and an east–west at the Mediterranean scale during the Holocene? (3) Is it possible to document, with accuracy, from pollen data, the seasonality of climate? In particular, the summer and winter parameters, as many studies diverge on the summer signal. Are the climate models (GCMs and regional) simulations in agreement with our results? (4) When and how did the Mediterranean conditions we know today come about?

In contrast to previous synthesis (Cheddadi et al., 1997; Davis et al., 2003; Mauri et al., 2014, 2015; Cruz-Silva et al., 2023; Liu et al., 2023), our study is based on a multi-method approach (e.g., Peyron et al., 2005; Brewer et al., 2008; Peyron et al., 2011, 2013, 2017; Salonen et al., 2019; Robles et al., 2022; d'Oliveira et al., 2023; Robles et al., 2023) applied to 38 fossil pollen records located in the north-central Mediterranean. Such an approach is more reliable than studies based on a single method (Chevalier et al., 2020). We will give particular attention to document the seasonality of temperature and precipitation interpretations because climate forcing during the Holocene was dominated by orbitally controlled insolation changes that operated asymmetrically across the annual cycle (Renssen et al., 2012). To increase the reliability of our reconstruction, a first stage of numerical tests (autocorrelation, canonical correspondence analysis) will be carried out on three modern climate and pollen datasets (global and regional) for annual and seasonal (spring, summer, autumn and winter) temperature and precipitation parameters.

Our results will be compared (1) to transient model simulations (TraCE-21Ka) from the Community Climate System Model (CCSM3; Collins et al., 2006) and (2) to the synthesis of Liu et al. (2023) for the Western Mediterranean and those of Cruz-Silva et al. (2023) for the Eastern Mediterranean to better understand the climate changes at the Mediterranean scale. The data-models comparison will give us a better understanding of climate mechanisms and their forcings.

https://doi.org/10.5194/egusphere-2025-1106
Preprint. Discussion started: 14 March 2025

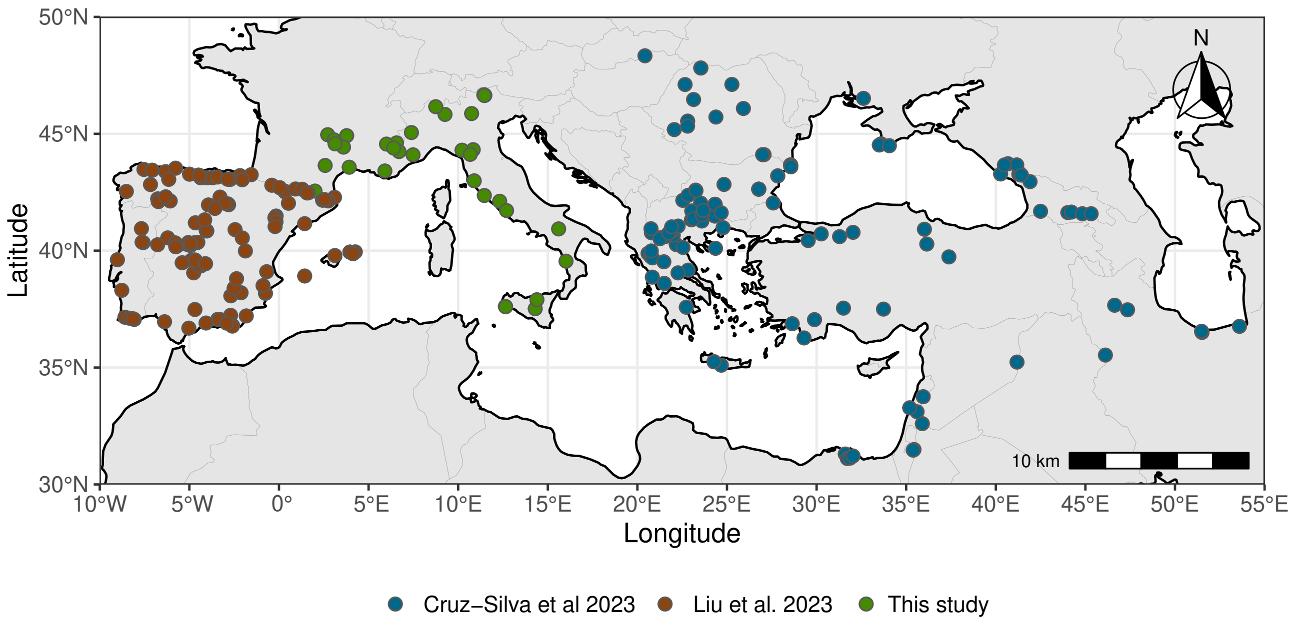

Figure 1. Spatial coverage of pollen-based Holocene climate syntheses for the northern Mediterranean basin focusing on the Iberian Peninsula (Liu et al., 2023), the Eastern Mediterranean (Cruz-Silva et al., 2023) and the north-central Mediterranean (this study).

https://doi.org/10.5194/egusphere-2025-1106
Preprint. Discussion started: 14 March 2025

2 Material and methods

2.1 Study area

The study region covers the north-central Mediterranean Basin (Fig. 2a) and is divided into two study zones, i.e., Southern France and Italy.

Zone 1 (Southern France) extends from the southern French coast to the north of the Massif Central, including part of the Pyrenees and the Alps and extends from longitude 1° E to longitude 8° E. This region is influenced by a Mediterranean climate, associated with cool mild winters and hot dry summers (Fig. 2b-c). Mean annual precipitation ranges from 500 to 800 mm, with a maximum recorded in autumn and a minimum in summer. Rainfall seasonality is influenced by altitude, resulting in an increase in spring precipitation with altitude while temperatures decrease (Azuara et al., 2020). Because of its latitude, southern France is directly influenced by large-scale atmospheric circulation patterns over the North Atlantic and Europe, i.e., a persistent low-pressure area located over Iceland, alongside the semi-permanent high-pressure system associated with the Azores (Brandimarte et al., 2011). Low-pressure conditions over Iceland, corresponding to an anticyclonic situation over the eastern Atlantic, will result in cold, dry and northerly wind over southern France, specifically over the Gulf of Lion, while a high-pressure situation will induce warm, humid and south-easterly winds (Azuara et al., 2020). The dynamic interplay between these two regions (i.e., Azores and Iceland) alters the westerly airflow patterns, impacting thermal exchanges across the North Atlantic and Europe, particularly during the winter months at mid to high latitudes (Brandimarte et al., 2011). Furthermore, the westerly flow exhibits inter-annual variability, oscillating between northern and southern trajectories.

This phenomenon, called the North Atlantic Oscillation (NAO), is most responsible for the inter-annual climate variability in the western Mediterranean. The NAO strength is measured by the difference between the normalised sea level pressure (SLP) recorded in the Atlantic at high and low latitudes. A positive NAO indicates an increased meridional pressure gradient, resulting in stronger westerly winds, whereas a negative NAO index suggests a decreased meridional pressure gradient, leading to weaker westerlies (Azuara et al., 2020). During positive NAO winters, there is an observed increase in atmospheric pressure across the subtropics, coupled with a decrease in pressure over the Arctic. This configuration results in a variety of winter weather patterns: Southern Europe experiences warmer and drier conditions, Northern Europe sees warmer and wetter weather, while Greenland endures colder and drier winters (Brandimarte et al., 2011).

Zone 2, corresponding to Italy, is located in the northern-central Mediterranean basin and stretches from latitude 36° N to latitude 47° N, which makes the climatic conditions very variable. The Italian orography is also very complex due to the presence of the Alps to the north and the Apennines, which stretches along the entire peninsula, acting as a barrier to air masses from continental Europe. Both mountain chains influence the pathway of weather fronts and interact with dominant winds, thereby exposing various regions of Italy to distinct circulation patterns (Fratianni and Acquaotta, 2017). The Alps act as a barrier, limiting the influx of cold air masses from central Europe into the Po Valley and northern Italy. The Apennines diminish the vulnerability of western areas to cold easterly winds that originate from the Balkans, while the Adriatic Sea, situated on the upwind side, is more susceptible to strong winds and heavy rainfall (Di Bernardino et al., 2024). The Italian Peninsula, surrounded by the Mediterranean Sea to the west, south and east, has its climate strongly mitigated by the presence

https://doi.org/10.5194/egusphere-2025-1106
Preprint. Discussion started: 14 March 2025

of the water body, which represents an important source of heat and moisture (Winschall et al., 2014). The simultaneous impact of multiple geographic elements (e.g., elevation, distance from the sea, presence of particular coastal currents, exposition to dominant winds etc.) shapes the presence of distinct climatic zones, each associated with particular prominence of weather types.

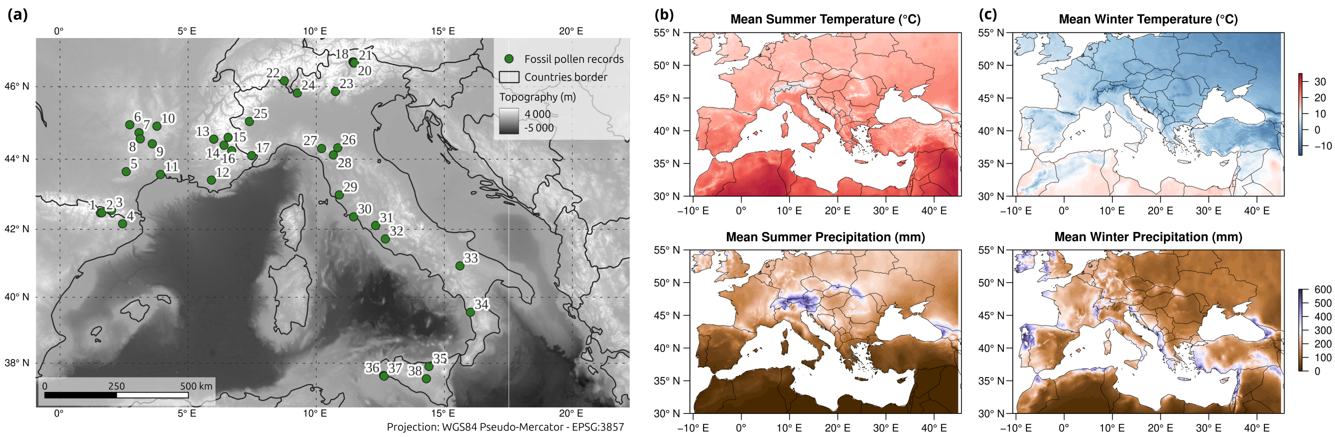

Figure 2. (a) Location of the 38 fossil pollen records used for palaeoclimate reconstruction. Current mean (b) summer and (c) winter temperature (top) and precipitation (bottom) repartition in the Mediterranean basin. Current climate parameters are based on average monthly climate data for 1970-2000 and extracted from WorldClim version 2.1 (Fick and Hijmans, 2017).

2.2 Pollen datasets

2.2.1 Fossil pollen data

Here, 38 pollen records, detailed in Tab. 1, were selected and extracted using the international database Neotoma (Williams et al., 2018) or gathered directly from the authors of the original studies. The pollen records were selected according to specific criteria such as location, temporal extent and resolution of each record. The aim was to compile the most suitable records for synthesising the Mediterranean climate of the Holocene (Fig. 2a).

The first selection criterion was the location, i.e., southern France (latitude 42–45° N; longitude 1–8° E) and Italy (latitude 37–47° N; longitude 8–16° E): 749 pollen records were selected and extracted from Neotoma. Before further restricting the selection, the LegacyAge 1.0 dataset (Li et al., 2022) was used to update the age–depth models of each record. The LegacyPollen database, compiled by Herzschuh et al. (2022), contains 2,831 pollen records from all over Europe, covering the last 30,000 years, whose pollen data and age models have been homogenised and updated. For the pollen data, the Neotoma data were retained because pollen homogenisation of the LegacyPollen database results in a loss of information due to the level of grouping of taxa, making the use of these homogenised pollen records impractical for the application of our multi-method approach to reconstructing climate change.

https://doi.org/10.5194/egusphere-2025-1106
Preprint. Discussion started: 14 March 2025

Once the age–depth models had been updated, the temporal extent was used as a second selection filter. For the two zones, the extent was set as follows: the pollen record must cover the period before 8,000 years cal. BP and after 5,000 years cal. BP and its signal must be continuous between 10,000–5,000 years cal. BP. The application of this constraint is intended to guarantee that any climate trend or oscillation that occurs can be documented. Finally, a last selection filter was applied by calculating the temporal resolution of each fossil record and then discarding the ones for which the mean resolution exceeds 350 years.sample^{-1}.

A total of 38 fossil pollen records were compiled for the two study zones, including 17 pollen records for southern France and 22 for the Italian peninsula (16 fossil pollen records from Neotoma and 5 directly from the authors of the original studies: Sadori and Narcisi, 2001; Mercuri et al., 2002; Joannin et al., 2012, 2013; Mercuri et al., 2013; Joannin et al., 2014b; Sadori, 2018).

During the ID dataset cross-referencing stage, selected records that are not recognised in the LegacyPollen database are temporarily extracted to check the pre-existing age models and recalculate them if necessary. The age–depth model of these sites was updated with the following procedure: the age models were calibrated and recalculated on R Studio (Team, 2020) with the `Bacon` package (Blaauw and Christen, 2011, version 3.3.0) using the IntCal20 calibration (Reimer et al., 2020) and based on their radiocarbon data available on Neotoma. A minimum of 4 radiocarbon dates was set, in line with the study by Li et al. (2022), to allow the pre-existing age–depth model to be updated. Records for which this constraint was unmet were removed from the fossil pollen dataset. In total, from the 38 fossil pollen records, only two age–depth models have to be recalculated.

The pollen data from the selected records were taxonomically homogenised (exclusion of aquatic taxa and spores). Herbaceous and woody taxa that were rarely observed were grouped into higher taxonomic categories, such as genus, sub-family, or family, following a thorough verification of their distribution within climate space.

For each record, the local environmental context was checked against the original publication (a time-consuming but necessary step) to highlight the presence of local hygrophilous and/or mesohygrophilous taxa (e.g., Cyperaceae, *Alnus glutinosa*-type, *Salix*, *Populus*). In certain records, it was necessary to eliminate these "local" taxa more characteristic of wetlands, such as shallow lakes and peat bogs (one record in Southern France and 11 records in Italy).

https://doi.org/10.5194/egusphere-2025-1106
Preprint. Discussion started: 14 March 2025

Table 1. Fossil pollen records used for the climatic reconstruction. Records are classified by zone (1: Southern France; 2: Italy) and by a west–east gradient for zone 1 and by a north–south gradient for zone 2.

ID	Sitename	Latitude (° N)	Longitude (° E)	Elevation (m)	Zone	Age min (yrs BP)	Age max (yrs BP)	Resolution (yrs.sple^{-1})	Modern dataset	Database	Reference
1	Planell de Perafita	42.48	1.57	2231	1	3091	10158	157.04	EAPDB	Neotoma	Miras et al. (2010)
2	Bosc dels Estanyons	42.48	1.63	2296	1	-55	11899	129.93	EAPDB	Neotoma	De Beaulieu et al. (2005); Miras et al. (2007)
3	Lake Racou	42.55	2.01	2014	1	284	12148	152.1	EAPDB	Neotoma	Guiter et al. (2005)
4	Les Palanques	42.16	2.44	465	1	39	8491	130.03	TEMPDB	Neotoma	Pérez-Obiol (1988); Piqué et al. (2018); Revelles et al. (2018)
5	Canroute	43.65	2.58	790	1	-77	12494	241.75	TEMPDB	-	d'Oliveira et al. (2023)
6	Peyre peat-bog	44.96	2.72	1097	1	308	12453	94.15	TEMPDB	Neotoma	Surmely et al. (2009)
7	Brameloup	44.74	3.08	1224	1	72	12499	146.2	TEMPDB	Neotoma	De Beaulieu et al. (1985)
8	Bonnecombe	44.57	3.13	1388	1	1698	12423	214.5	TEMPDB	Neotoma	De Beaulieu et al. (1985)
9	Tourbiere des Narses Mortes	44.43	3.6	1256	1	-20	10671	334.09	TEMPDB	Neotoma	de Beaulieu (1974)
10	Lac du Bouchet	44.92	3.78	1181	1	-47	12324	268.93	TEMPDB	Neotoma	Reille and De Beaulieu (1988); Thouveny et al. (1990)
11	Embouchac	43.57	3.92	9	1	1461	9417	42.32	TEMPDB	Neotoma	Puertas (1998, 1999)
12	Tourves	43.41	5.91	304	1	1582	16035	123.53	TEMPDB	Neotoma	Nicol-Pichard (1987)
13	Correo	44.56	6	1101	1	662	12496	81.61	TEMPDB	Neotoma	Nakagawa (1998)
14	Vallon de Provence	44.39	6.4	2075	1	2891	11809	107.45	EAPDB	Neotoma	De Beaulieu and Jorda (1977)
15	Lac de Siguret	44.61	6.56	1066	1	3879	12408	213.23	TEMPDB	Neotoma	De Beaulieu and Jorda (1977); Beaulieu and Reille (1983)
16	Plan du Laus	44.24	6.7	1783	1	922	11978	155.72	EAPDB	Neotoma	De Beaulieu and Jorda (1977)
17	Lac des Grenouilles	44.1	7.48	1810	1	2177	12159	133.09	EAPDB	Neotoma	Finsinger et al. (2021)
18	Schwarzsee	46.67	11.43	2033	2	34	11600	131.43	EAPDB	Neotoma	Seiwald (1979)
19	Malschotscher Hotter	46.67	11.46	2050	2	0	11492	208.95	EAPDB	Neotoma	Seiwald (1979)
20	Dura Moor	46.64	11.46	2080	2	7	12461	125.8	EAPDB	Neotoma	Seiwald (1979)
21	Rinderplatz	46.64	11.49	1780	2	-7	12374	113.59	EAPDB	Neotoma	Seiwald (1979)
22	Balladrum	46.16	8.75	390	2	-30	12358	176.97	TEMPDB	Neotoma	Hofstetter et al. (2006)
23	Lago di Ledro	45.87	10.75	652	2	10	18156	92.11	TEMPDB	-	Joannin et al. (2013, 2014b)
24	Lago del Segrino	45.83	9.26	374	2	-19	12166	133.9	TEMPDB	Neotoma	Gobet et al. (2000)
25	Lago Piccolo di Avigliana	45.05	7.39	356	2	331	12478	36.59	TEMPDB	Neotoma	Finsinger and Tinner (2006); Finsinger et al. (2011)
26	Pavullo nel Frignano	44.32	10.84	675	2	50	12341	279.34	TEMPDB	Neotoma	Vescovi et al. (2010a)
27	Lago Padule	44.3	10.21	1187	2	-10	11834	171.65	TEMPDB	Neotoma	Watson (1996)
28	Lago del Greppo	44.12	10.67	1442	2	-60	11031	96.44	TEMPDB	Neotoma	Vescovi et al. (2010b)
29	Lago dell'Accesa	42.99	10.9	157	2	261	11842	87.73	MEDDB	Neotoma	Drescher-Schneider et al. (2007)
30	Lago di Mezzano	42.36	11.46	452	2	67	15309	127.02	TEMPDB	-	Sadori (2018)
31	Lago di Martignano	42.11	12.32	200	2	83	12599	184.06	TEMPDB	Neotoma	Kelly and Huntley (1991)
32	Lago di Nemi	41.72	12.7	320	2	3.1	11386	130.84	MEDDB	-	Mercuri et al. (2002, 2013)
33	Lago Grande di Monticchio	40.93	15.61	656	2	87	12436	138.75	TEMPDB	Neotoma	Allen and Huntley (2018)
34	Lago Trifoglietti	39.55	16.02	1048	2	14	11439	69.24	TEMPDB	-	Joannin et al. (2012)
35	Urio Quattrocchi	37.9	14.4	1044	2	3154	10348	78.2	MEDDB	Neotoma	Bisculm et al. (2012)
36	Lago Preola	37.62	12.63	6	2	-46	10366	160.18	MEDDB	Neotoma	Calò et al. (2012)
37	Gorgo Basso	37.6	12.65	6	2	-57	10501	121.36	MEDDB	Neotoma	Tinner et al. (2009)
38	Lago di Pergusa	37.52	14.3	667	2	53	12749	156.74	MEDDB	-	Sadori and Narcisi (2001)

https://doi.org/10.5194/egusphere-2025-1106
Preprint. Discussion started: 14 March 2025

2.3 Modern pollen data

Different studies underline the importance of the modern pollen and climate datasets used (Turner et al., 2021) and some of them point out the advantage of regional datasets (Dugerdil et al., 2021a, b). To test the role of the modern dataset on the reconstruction (Trasune et al., 2024), and improve the reliability of our climate reconstructions, three modern pollen datasets were used, one global and two regional. The Eurasian Pollen Dataset (EAPDB), compiled by Peyron et al. (2013, 2017) and updated by Dugerdil et al. (2021a) and Robles et al. (2022, 2023), was used as the global modern pollen dataset. The EAPDB contains a total of 3,373 pollen surface samples (Fig. A1a). The two regional modern datasets are derived from a sub-sample of the EAPDB, and correspond to a temperate pollen dataset (TEMPDB) and a Mediterranean pollen dataset (MEDDB). The TEMPDB corresponds to the temperate European region, samples from the EAPDB were extracted using both a spatial selection (Western Europe) and a temperate biome selection (warm mixed forest, xerophytic wood/shrub, temperate deciduous forest, cool mixed forest, warm steppe, cold mixed forest, cool steppe). Similarly to the TEMPDB, the MEDDB is the result of a resampling of the EAPDB by a spatial selection (the Mediterranean basin) and a selection by biomes (warm mixed forest, xerophytic wood/shrub, temperate deciduous forest, warm steppe, cold mixed forest, cool mixed forest). After compiling the two regional datasets, the TEMPDB and the MEDDB contain 1,875 and 1,040 surface pollen samples respectively (Fig. A1b-c). For the three modern pollen datasets (EAPDB, MEDDB and TEMPDB) a total of 103 taxa were used. Taxa representing less than 0.1 % of the pollen spectra at a given site were removed.

For each modern pollen sample, seasonal and annual climate values were extracted from the WorldClim2.1 dataset (Fick and Hijmans, 2017) as follows: Mean annual temperature (MAAT), spring temperature (Tspr), summer temperature (Tsum), autumn temperature (Taut), winter temperature (Twin), mean annual precipitation (MAP), spring precipitation (Pspr), summer precipitation (Psum), autumn precipitation (Paut) and winter precipitation (Pwin).

The modern dataset used for each fossil record was adapted according to the dominant taxa, and regional datasets (TEMPDB and MEDDB) were used whenever possible. The MEDDB was selected when at least 15% of Mediterranean taxa (*Olea, Phillyrea, Pistacia* and *Quercus ilex*-type) were present in the record, otherwise, the TEMPDB was selected. Where certain mountainous/boreal taxa such as *Picea* or *Betula* were dominant ($\geq$ 75%) the global EAPDB dataset was selected to limit the no-analogue situations. To facilitate the identification of climatic trends, the records were organised along a longitudinal west–east gradient for southern France and a north–south latitudinal gradient for Italy. The potential biases linked to the elevation of the sites (Ortu et al., 2006) were also investigated, and the fossil records have been distinguished as low (< 1000 m) and high ($\geq$ 1000 m) elevations.

2.4 A multi-method approach to reconstruct past climate from pollen data

Over the last decades, several methods have been developed to reconstruct climate from pollen data (see review by Chevalier et al., 2020). As these methods are based on different ecological concepts and mathematical algorithms, results can be strongly method-dependent (Chevalier et al., 2020). In this frame, multi-method approaches have been developed to increase the reliability of the results (Peyron et al., 2005, 2011, 2013, 2017; Salonen et al., 2019; Robles et al., 2022, 2023; Sassoon et al.,

https://doi.org/10.5194/egusphere-2025-1106
Preprint. Discussion started: 14 March 2025

2025). These methods were initially developed to calibrate the relationship between modern pollen data (soils, mosses) and current climate parameters. Multi-method approaches include (1) assemblages approach, based on the principle of dissimilarity between fossil and modern assemblages (Modern Analogue Technique); (2) transfer functions, based on linear or non-linear regressions (Weighted Averaging Partial-Least Squares regression) between pollen taxa and climate parameters, and (3) recent machine learning techniques with regression trees (Random Forest and Boosted Regression Trees) to quantify climate parameters.

The Modern Analogue Technique (MAT; Guiot, 1990), is widely used to reconstruct past climates due to its straightforward application, efficacy, and sensitivity. This technique relies on evaluating the dissimilarity between each fossil and modern pollen assemblages, and by selecting the closest modern samples (known as analogues). The WA-PLS method, introduced by ter Braak and Juggins (1993), operates as a transfer function that assumes an unimodal relationship between the proportions of pollen and climatic conditions. It suggests that the abundance of a species is intrinsically linked to its environmental tolerance. WA-PLS calculates the climatic optimum for a species based on calibration data by determining the average climatic conditions in which the species is found, weighted according to its abundance (Chevalier et al., 2020).

The two additional methodologies, namely Random Forest (RF) and Boosted Regression Trees (BRT), have emerged more recently and are grounded in Machine Learning principles (Salonen et al., 2019). These techniques utilise regression trees to systematically partition pollen data through successive divisions based on the abundance observed in the pollen spectrum. The Random Forest approach relies on the estimation and aggregation of multiple regression trees, with each tree being derived from a collection of pollen samples using a bootstrapping technique (Chevalier et al., 2020). In contrast, Boosted Regression Trees differ from RF in their treatment of the modern dataset: while RF assigns equal selection probabilities to all samples, BRT increases the likelihood of selecting under-represented samples from the previous tree. This technique, known as boosting, enhances the model's predictive accuracy for elements that are less accurately predicted (Salonen et al., 2019). Here, the final output of the BRT method is derived from averaging the results of 15 independent executions of the BRT algorithm, reflecting the variability inherent in regression tree signals.

For each method, the reliability of the results was estimated by bootstrap cross-validation by calculating the values of the correlation coefficient between the variables (R^2) and those of the root mean square error criterion (RMSE).

2.5 Numerical analyses

The relationships between climate variables were assessed with a scatter-plot matrix to provide an overview of the distributions and correlations of the variables and were pair-plot drawn.

To assess the relationships between modern pollen spectra and the climatic variables an ordination technique was used on each modern pollen dataset. Major pollen taxa (those present in a least 15 samples and with a maximum $\geq$ 3%) of each dataset were square-root-transformed to stabilise variances and optimise the signal-to-noise ratio (Prentice, 1980). A detrended correspondence analysis (DCA; Hill and Gauch, 1980) was applied to each modern pollen dataset to determine whether a linear-based analysis or unimodal-based analysis was more appropriate based on gradient length as the criterion. The DCA results

https://doi.org/10.5194/egusphere-2025-1106
Preprint. Discussion started: 14 March 2025

showed that, for the three modern datasets, the gradient length was over 3.0 standard deviation, suggesting that unimodal-based methods should be used in further analyses on the modern pollen datasets (Ter Braak and Verdonschot, 1995).

A canonical correspondence analysis (CCA) was carried out to detect the influence of climate variables on each modern pollen dataset, and variance inflation factors (VIFs) were also used to determine the correlations between environmental variables. VIF values > 10 indicate co-linearity with other variables, which may lead to unreliable results (Ter Braak and Prentice, 1988; Cao et al., 2014). To eliminate the correlation between the variables, we selected the temperature and precipitation variables with a large explained variance and eliminated those with a VIF > 10.

Climate reconstructions based on different methods and reliability tests (R^2 criterion and RMSE) were performed with the packages `rioja` (Juggins, 2024, version 1.0.7), `randomForest` (Breiman, 2001, version 4.7-1.2) and `dismo` (Hijmans et al., 2024, version 1.3.16). All analyses were performed on R Studio (Team, 2020, version 4.4.1), using the `ggplot2` package (Wickham, 2016, version 3.5.1) for graph creation.

To facilitate the comparison of climate signals between each record and the identification of potential patterns of changing climate trends between records, a normalisation between -1 and 1 (rescaling min-max) is applied to the smoothing of the mean of selected models for each record. Data normalisation is based on the following equation Eq. (1):

$$x^{'} = a + \frac{(x - min(x))}{(max(x) - min(x))} \times (b - a) \tag{1}$$

With x non-smoothed initial mean values, $x^{'}$ normalised smoothed values, a and b minimal and maximal normalisation values, in this case respectively -1 and 1.

To not bias this representation toward drier or warmer values, the period for which the impact of human activity is discernible in the pollen diagrams, have been excluded from the standardisation process. The exclusion is either based on the author's fossil record note gathered during the compilation directly from the original publication or on a significant percentage of specific anthropic taxa such as: *Juglans*, *Castanea*, *Olea*, *Cerealia*-type, *Plantago lanceolata*, and *Rumex*-type.

Composite curves are constructed for the central Mediterranean area and will be compared to other palaeoclimate syntheses of the Mediterranean region (Cruz-Silva et al., 2023; Liu et al., 2023). For the composite curves, non-normalised reconstruction results were used, without the exclusion of periods where the human activity is discernible. Reconstructed palaeoclimate values of every climate parameter were averaged in a 300 year bin, the maximal resolution of all records being 306 years. For each record, the first bin was centred on 0 years BP, and the following bins were centred on a 300 year increment throughout the record. Then the binned values of each record were averaged to produce a regional climate signal for the central Mediterranean. Finally, the regional climate signal values were transformed into anomalies, the anomaly calculation is based on the reconstructed modern average value. The estimation of confidence intervals for each composite, encompassing the 5th and 95th percentiles, was achieved through bootstrap resampling at the site level, utilising 1000 iterations.

https://doi.org/10.5194/egusphere-2025-1106
Preprint. Discussion started: 14 March 2025

3 Results

3.1 Ordinations

The pair-plots of the ten climatic variables for all three modern pollen datasets (Fig. A2) indicate that mean annual temperature (MAAT) and precipitation (MAP) are highly correlated (Pearson correlation coefficient > 0.7) with the seasonal parameters (Taut, Tspr, Twin, Tsum and Paut, Pspr, Pwin, Psum). Among seasonal parameters, spring (Tspr and Pspr) and autumn (Taut and Paut) parameters are the ones which are also highly correlated between them. This co-linearity is supported by the canonical correspondence analyses (CCAs) of the pollen assemblages and the climate variables for the three modern datasets (Fig. 3). For each modern pollen dataset, the first CCA, with every climate parameter, indicated that the variance inflation factor (VIF) values of annual (TANN, PANN), spring (Tspr and Pspr) and autumn (Taut and Paut) parameters are greater than 10 (Fig. 3a-c). After deleting those parameters, the remaining four climate variables (Tsum, Twin, Psum and Pwin) have VIF values lower than 10 and, therefore, can be used in the final CCA to investigate their influence on modern pollen datasets (Fig. 3d-f).

https://doi.org/10.5194/egusphere-2025-1106
Preprint. Discussion started: 14 March 2025

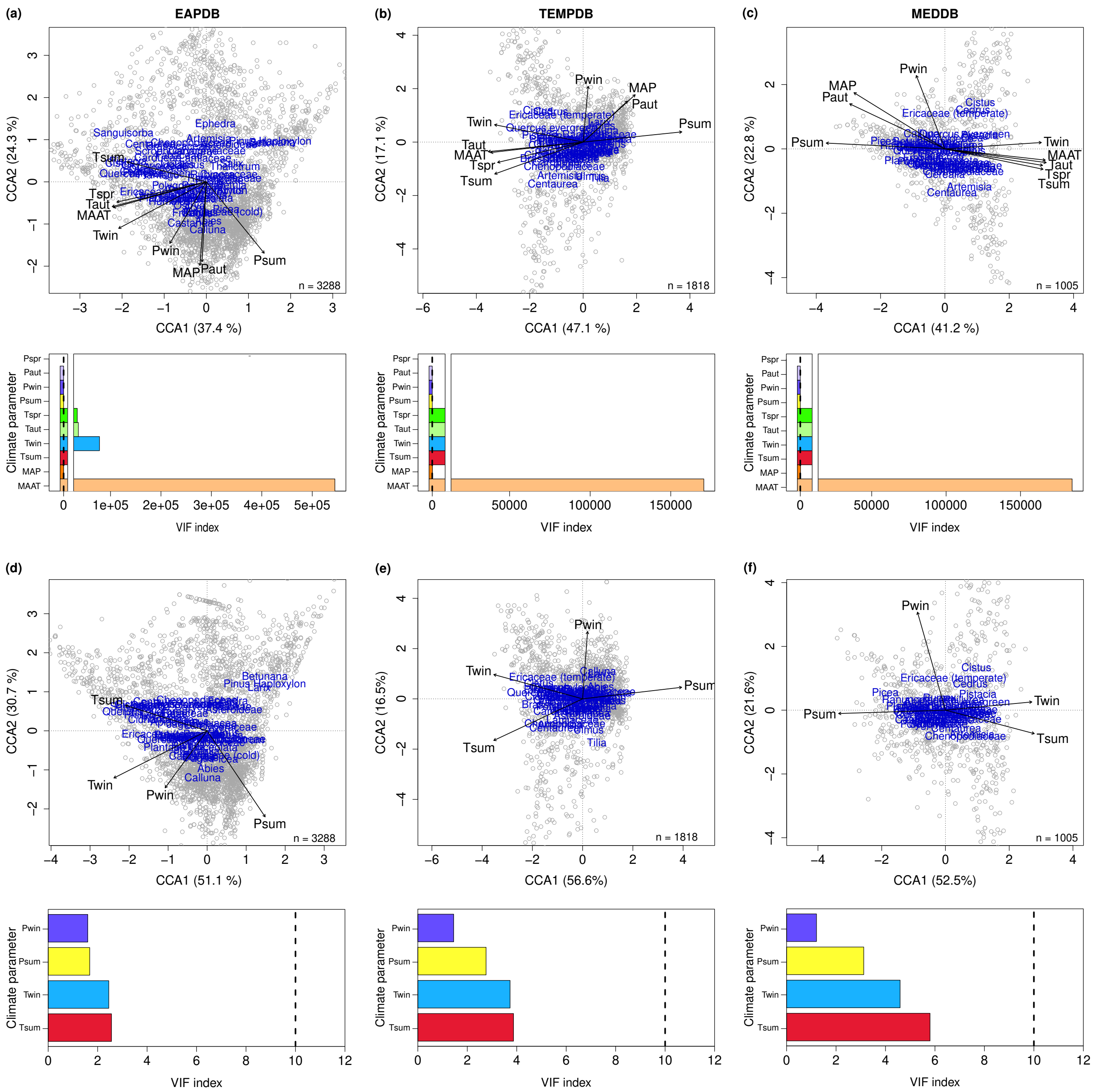

Figure 3. Canonical Correspondence Analysis (CCA) results and Variance Inflation Factor (VIF) values for (a and d) the Eurasian Pollen Database (EAPDB), (b and e) the Temperate Pollen Database (TEMPDB) and (c and f) the Mediterranean Pollen Database (MEDDB). The variance of axis 1 (CCA1) and axis 2 (CCA2) is expressed in percentages on the axis label. Panels (a) to (c) correspond to (top) the first canonical correlation analysis (CCAs) and (bottom) VIF values applied to all climate variables. Panels (d) to (f) correspond to (top) the second canonical correlation analysis and (bottom) VIF values without climate variable with VIF values > 10. Dashed lines mark the threshold of 10 used to on VIF values determine the presence of correlation between the environmental variables.

https://doi.org/10.5194/egusphere-2025-1106
Preprint. Discussion started: 14 March 2025

290 ## 3.2 Model performances

Results of model performances, estimated by bootstrap cross-validation, are summarised in Fig. 4 with the correlation coefficient (R^2, Fig. 4a) and the root mean square error criterion (RMSE, Fig. 4b1b2). For all climate parameters, and all modern datasets, best R^2 and RMSE values, i.e., respectively highest and lowest values, are obtained for MAT and BRT methods. Conversely, the WA-PLS and RF methods show lower R^2 and RMSE values. Therefore, we will retain here the MAT and BRT
295 methods for the interpretation and discussion of our climate reconstructions.

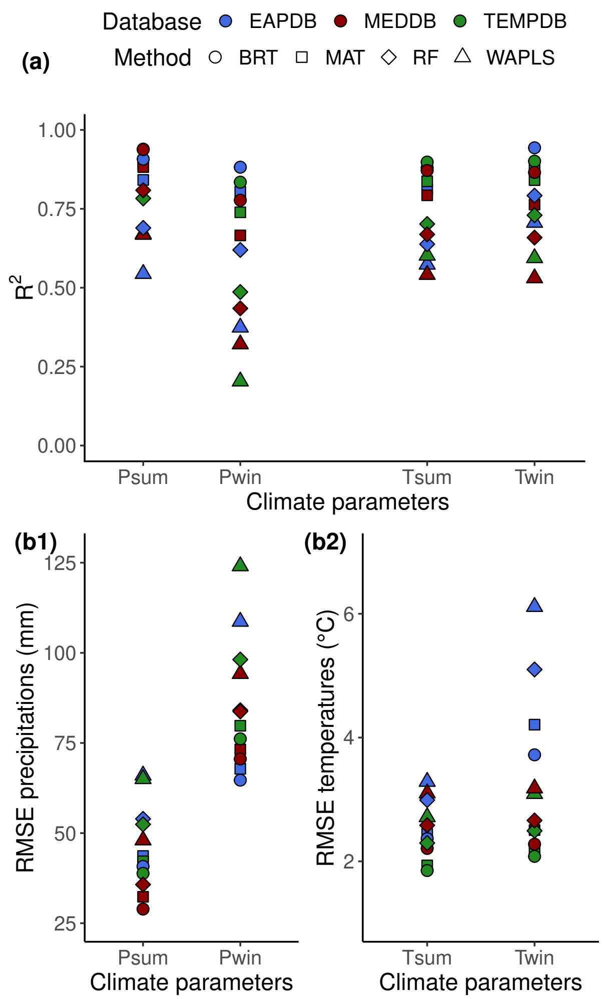

Figure 4. Performance results of the four methods tested (MAT, WA-PLS, BRT, and RF) with the three different modern pollen datasets – the modern Eurasian (EAPDB), Temperate (TEMPDB), and Mediterranean (MEDDB) datasets – for summer and winter precipitation (Psum, Pwin) and temperature (Tsum, Twin). (a) R-squared values (R^2). (b1) Root Mean Square Error of precipitations (RMSE). (b2) Root Mean Square Error of temperatures (RMSE).

https://doi.org/10.5194/egusphere-2025-1106
Preprint. Discussion started: 14 March 2025

3.3 Quantitative palaeoclimate reconstructions

The MAT and BRT were applied to each fossil pollen record to reconstruct the summer and winter climate parameters (Figs. 5 and 6). To compare more easily the different sequences, the results obtained with both methods were averaged for each record. This averaged signal was then normalised (rescaling min-max method, Eq. (1)) according to the mean value of the smoothed climatic signal for the entire record.

3.3.1 Summer conditions: temperature and precipitation

Southern France was influenced by a west–east temperature gradient (Fig. 5a). The western and central regions of zone 1 (records 1 to 11) are characterised by a downward trend in summer temperatures during the Holocene. Tsum were relatively high from the beginning of the Holocene to around 6,000 years cal. BP before falling until the modern period. This climatic pattern, particularly evidenced in the high elevation records, suggests the presence of a Holocene Thermal Maximum (HTM) in these regions. For the more easterly regions of southern France (records 12 to 17), an opposite pattern appears to be present, with higher summer temperature trends toward the most recent period. In Italy, summer temperatures seem to be strongly influenced by a north–south division with different patterns, distributed on either side of latitude 43° N. The region of zone 2 located above 43° N (records 18 to 28) is characterised by two different patterns depending on high or low elevation (Fig. 5a). At high elevations (records 18 to 21 and 27 to 28), high summer temperature values are reconstructed from the beginning of the Holocene to around 6,000 years cal. BP before falling until the recent period. This pattern is similar to the one observed at high elevations in southern France, also suggesting the presence of an HTM in the Italian Alps. At lower elevations (records 22 to 26), low summer temperature values are evidenced from the beginning of the Holocene to around 5,000 years cal. BP, followed by a summer warming to the modern-day period. Below 43° N, an opposite climatic pattern to that at low elevation is present, corresponding to relatively low Tsum values at the beginning of the Holocene, followed by an increase from 8,000 years cal. BP onward, which continues into modern times.

For summer precipitation (Psum), three patterns, depending on a west–east gradient, are evidenced in southern France (Fig. 5b). In the westernmost region of zone 1 (records 1 to 4), high precipitations are reconstructed between the early and mid Holocene periods (around 9,000–4,500 years cal. BP). A decrease in summer precipitation occurs during the late Holocene, more or less early depending on the record, suggesting summer aridification throughout the Holocene. In contrast, records from the central region of southern France (records 5 to 11) indicate dry conditions during the early Holocene, followed by a wetter mid to late Holocene. High-elevation sequences highlight a precipitation maximum earlier and longer (around 8,000–4,000 years cal. BP) than the low-elevation sequences (6,000–3,000 years cal. BP). Further east (records 11 to 17), we reconstruct a pattern similar to that observed for the western regions of southern France (high precipitation followed by an aridification) but with an earlier and shorter humid period, i.e., wetter conditions present during the early Holocene period (12,000–8,000 years cal. BP) before aridification from the onset of mid Holocene onward. In Italy, similarly to summer temperatures, summer rainfall is strongly influenced by a north-south gradient. Very contrasting climatic patterns are highlighted on either side of latitude 43° N. Above 43° N, low precipitations are reconstructed during the early Holocene until the onset of the mid

https://doi.org/10.5194/egusphere-2025-1106
Preprint. Discussion started: 14 March 2025

Holocene (12,000–8,000 years cal. BP), followed by high precipitation throughout the mid-to-late Holocene. Wetter summers are evidenced between 7,500 and 4,500 years cal. BP. In contrast, below 43° N, an opposite precipitation trend is reconstructed, with wet summers during the early Holocene (with a maximum around 9,000 years cal. BP), followed by drier conditions throughout the Holocene (particularly evidenced after 7,000 years cal. BP).

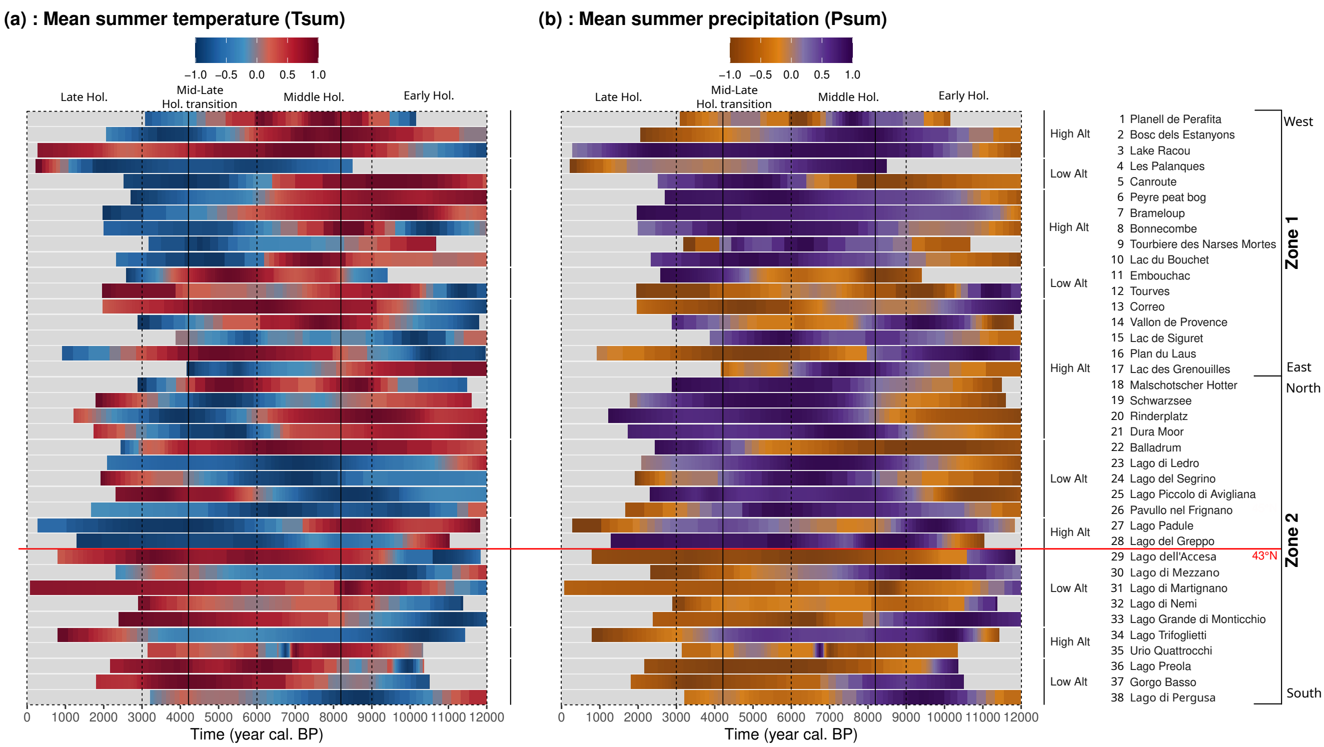

Figure 5. Summer (a) temperature (Tsum) and (b) precipitation (Psum) reconstructed from 38 fossil pollen records. The colour gradient corresponds to models-averaged min-max normalised values of each climate parameter. Positive (negative) values correspond to summer conditions that are (a) warmer (colder) and (b) wetter (drier) than the mean value of the climate signal for each record.

https://doi.org/10.5194/egusphere-2025-1106
Preprint. Discussion started: 14 March 2025

3.3.2 Winter conditions: temperature and precipitation

In zone 1, two distinct patterns are reconstructed (Twin, Fig. 6a). In the western and eastern regions of southern France (records 1 to 3 and 12 to 17) cold winter conditions occurred at the beginning of the Holocene, followed by warmer conditions. In the west (records 1 to 3) warmest conditions occur from the middle Holocene (8,000 years cal. BP) onward. In the east (records 12 to 17) the warming happens earlier and seems to last longer, from the early Holocene to the mid-to-late Holocene transition periods (around 11,000–5,000 years cal. BP) depending on the record. The central region of southern France (records 5 to 11), on the other hand, shows a more contrasted climatic signal, characterised by warm conditions during the early Holocene, followed by a temperature decrease during the mid Holocene before an increase until the modern period. In Italy, the winter climate signal seems much less influenced by the north–south division than in summer. The contrasting conditions observed in summer around 43° N are not depicted here, the climate signal is more homogeneous. Most of Italy is characterised by cold conditions during the early Holocene, followed by a gradual increase in winter temperatures throughout the Holocene.

For precipitation trends, we observed a spatial repartition similar to winter temperatures in southern France (Fig. 6b). The eastern and western regions of zone 1 (records 1 to 3 and 12 to 17) are defined by the same trends, i.e., an increase in winter precipitation over the Holocene, with wetter conditions observed from the mid Holocene period (8,000 years cal. BP) onward. In the central regions of southern France (records 5 to 11), Fig. 6 also suggests a winter precipitation increase although (1) the climatic signal seems more contrasted between the records, (2) the wetter conditions are observed later, during the mid-to-late Holocene transition period (between 5,000–3,000 years cal. BP), than in the other two regions of zone 1.

In the Alpine part of Italy and the northern Apennines (records 18 to 28), a similar pattern to that observed in the eastern part of southern France is evidenced, i.e., an increase in winter precipitation during the Holocene. However, the onset of wetter winter conditions seems to have been delayed at high altitudes (records 18 to 21). At lower elevations (records 23 to 25), the wet conditions occur earlier, during the early Holocene period (around 10,000 years cal. BP). In central Italy, in the regions of southern Tuscany and Lazio (records 29 to 32), there appears to be a general trend in winter throughout the Holocene, similar to that observed in northern Italy, i.e., a gradual increase in precipitation over the Holocene, with a stronger temporal heterogeneity between records. In Sicily (records 35 to 38), dry conditions are evidenced at the start of the Holocene until around 8,000 years cal. BP, followed by wetter conditions during the middle Holocene period (around 7,000 years cal. BP depending on the record).

https://doi.org/10.5194/egusphere-2025-1106
Preprint. Discussion started: 14 March 2025

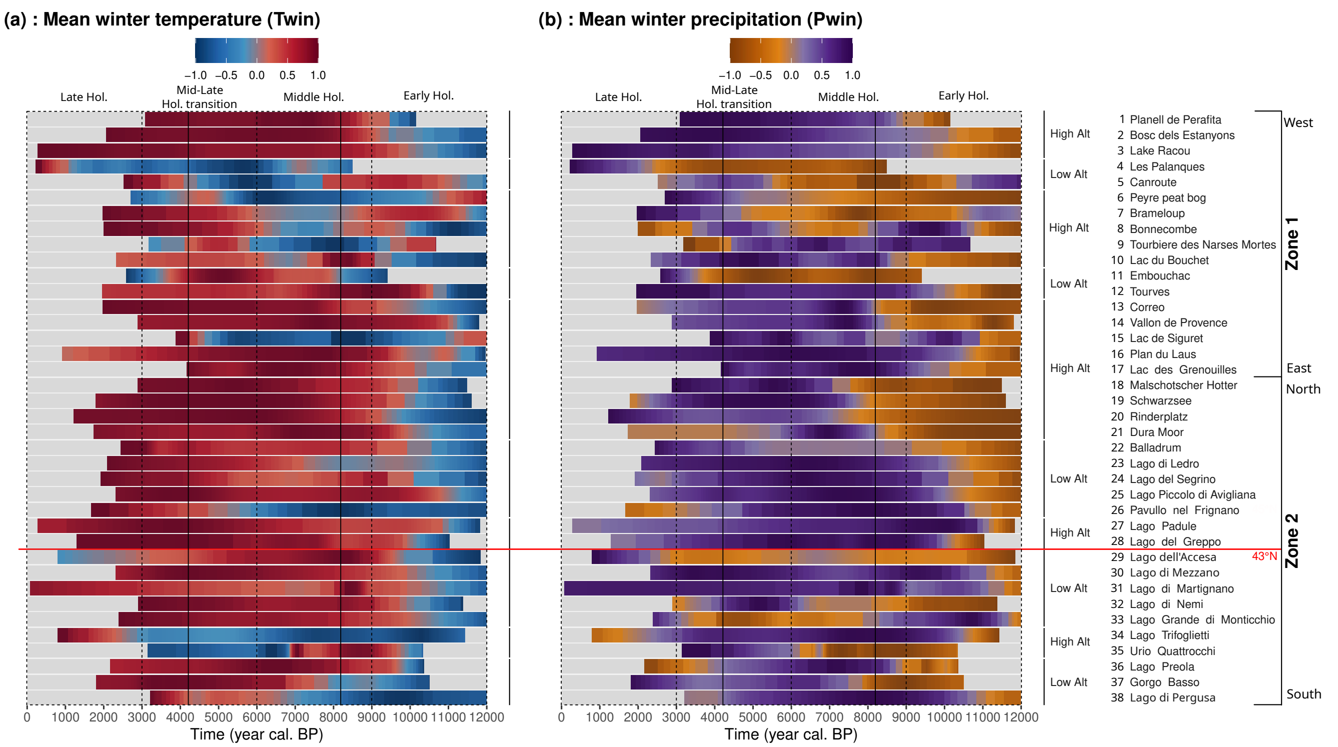

Figure 6. Winter (a) temperature (Twin) and (b) precipitation (Pwin) inferred from the 38 fossil pollen records. The colour gradient corresponds to models-averaged min-max normalised values of each climate parameter. Positive (negative) values correspond to winter conditions that are (a) warmer (colder) and (b) wetter (drier) than the mean value of the climate signal for each record.

https://doi.org/10.5194/egusphere-2025-1106
Preprint. Discussion started: 14 March 2025

4 Discussion

We used a pollen-inferred multi-method approach (3 modern datasets, 2 methods) to reconstruct specifically the climate changes in the central Mediterranean area over the last 12,000 years BP, with a focus on the seasonality estimates (temperature and precipitation of both winter and summer conditions). Results suggest that local/regional trends differ in the central Mediterranean during the Holocene. Summer conditions were characterised by a west–east distinction in southern France and a north–south one in Italy, for both temperature and precipitation. The HTM in summer has been found north of 43° N at high elevation ($\geq$ 1000 m). In contrast, Holocene winter conditions showed a more homogeneous spatio-temporal pattern, i.e., general wetter conditions and warming through the Holocene in both Italy and southern France, although some local discrepancies can be evidenced depending on the elevation of the site.

4.1 Importance of chronological considerations

We discuss here the chronology range, quality and resolution for each record, which are particularly important as they may induce some biases in the interpretation of the climatic reconstructions. For this study, specific criteria were applied to select records with a fairly good chronology, i.e., a continuous temporal range between 10,000 and 5,000 years cal. BP and an average temporal resolution of less than 350 years.sample^{-1}. However, it should be pointed out that the quality of the chronologies is not equal between each fossil pollen record, which may initially affect the accuracy of the reconstructions, but also the interpretation that will be made of them and can be considered as an unavoidable limitation in our reconstructions.

Another chronological concern is linked to the partitioning of Holocene climatic trends. Certain climatic periods that are emblematic of the Holocene in Europe, such as the Holocene Thermal Maximum (HTM), are not always identified at the same time and/or with the same intensity, for reasons that may depend on chronology, proxy sensitivity (marine vs terrestrial) and/or local response to climatic change (e.g., elevation, Bini et al., 2019). This is why the time interval definition is not always a simple or obvious choice. Divisions specific to the Mediterranean region have been proposed, notably by Jalut et al. (2000) who proposed a division into three periods with (1) a lower humid Holocene (11,500–7,000 years cal. BP), (2) a transition phase (7,000–5,000 years cal. BP) and (3) an upper Holocene (5,500 years cal. BP–present) characterised by aridification.

In contrast to the aforementioned study and to better discuss the climate changes of the central Mediterranean area in terms of spatio-temporal patterns, we choose to divide the Holocene into four periods: (1) 12,000–8,000 years cal. BP corresponding to the Lateglacial and early Holocene, (2) 8,000–5,000 years cal. BP during which the HTM should be observable if recorded, (3) 5,000–3,000 years cal. BP associated with post-HTM conditions and (4) 3,000 years cal. BP–present during which the human impact on vegetation is recorded in most of fossil pollen records.

4.2 Pollen-inferred uncertainties to be taken into account for Holocene palaeoclimate reconstructions in the Mediterranean region

Among the uncertainties that can impact our palaeoclimatic reconstructions, it seems essential to address the limitations of the pollen proxy when used in palaeoclimatic quantification. One of the first uncertainty that can be stated is the effect of the

https://doi.org/10.5194/egusphere-2025-1106
Preprint. Discussion started: 14 March 2025

agglomeration of several archive types (e.g., lakes and peat bogs) with different local recording conditions (e.g., sediment accumulation rate, edaphic conditions, hydroseral succession). Variability in spatial representativeness can affect the reconstructed palaeoclimatic signal, e.g., a lake associated with a small catchment will record a more local signal than a lake associated with a large catchment, which would better represent regional vegetation (Sugita, 1993; Herzschuh et al., 2023b). A second factor, a migrational lag, can impact our reconstructions based on pollen data, as vegetation can take time to return to equilibrium with its environment after a major and rapid climate change (Mauri et al., 2015). The impact of the migrational lag is generally considered for the Lateglacial–early Holocene transition, which corresponds to the last rapid climate shift of the last 12,000 years BP, when most of the postglacial vegetation began to take hold and before climate changes became less strong and less rapid. This uncertainties could impact the reconstructions of the Lateglacial and early Holocene periods of our study. Finally, it seems essential to address the impact of human presence and its interaction with vegetation when pollen data are used to reconstruct palaeoclimates. Several studies have already shown that human activity, through land clearance for grazing or cultivation, can lead to an over-representation of non-arboreal pollen, and thus influence palaeoclimate reconstructions in which vegetation changes do not entirely correspond to climatic variations (Birks et al., 2010; Mauri et al., 2015). In the central Mediterranean, studies showed that the main cause of vegetation changes before 4,000 years BP was climatic variations but after from the late Holocene onward, vegetation changes seemed to be attribute to human activity and climatic influences altogether (Sadori et al., 2011; Marignani et al., 2017). For our study, the modification of vegetation by humans is a point to be taken into account for palaeoclimate interpretations since the presence of anthropogenic taxa (i.e., *Juglans*, *Castanea*, *Olea*, *Cerealia*-type, *Plantago lanceolata* and *Rumex*-type) is observed in several records of zone 1 and 2 from around 3,000 years BP onward.

Studies have highlighted the importance of site effects on the response to climate change, such as complex topography and elevation, which can act as important perturbation factors to large-scale atmospheric flows (Beniston et al., 1997). The study by Ortu et al. (2010), focused on the Alps, showed that differences in the pollen assemblages of high ($\geq$ 1000 m) and low (< 1000 m) elevation sites play a significant role in the quality of climate reconstructions based on pollen. In our study, elevation seems to also play a role as the HTM observed in the south of France and the Italian Alps is best recorded at high elevations north of 43° N. However, this interpretation may be questioned because most pollen located north of 43° N is located at high elevations (19 out of 28 records). A greater number of high-elevation records south of 43° N would enable us to refine our climate interpretation, particularly in the south of France, where continuous pollen records are lacking.

4.3 A north–south climate division of the Italian Peninsula

The pioneering study by Magny et al. (2012, 2013) has first highlighted a north–south palaeohydrological contrast in the central Mediterranean during the Holocene. In addition, they identified a latitudinal "tipping point" around 40° N (Magny et al., 2013), splitting and distinguishing two distinct and opposite patterns on either side of latitude 40° N. In contrast to the study of Magny et al. (2013), which is based on 6 records, with only one record located between latitude 40 and 45° N, our synthesis is based on 38 records, 22 of which are located along the Italian Peninsula, giving us a unique opportunity to see whether the same north–south division also appears in our results at a wider scale. Here, a latitudinal division on either side of 43° N in Italy throughout the Holocene is evidenced in summer while winter climate conditions appear to have been more spatially

https://doi.org/10.5194/egusphere-2025-1106
Preprint. Discussion started: 14 March 2025

homogeneous and rather be marked by a stronger temporal dynamic (Fig. 5, 6, A3, A4). Our study corroborates the findings of Magny et al. (2013) but suggests that the "tipping point" takes place at higher latitudes, around 43° N, and only impacts summer climate conditions (Fig. 5, A3). Through a multi-proxy study, Robles et al. (2023) also highlighted a north–south climate division in Italy during the Lateglacial period, proposing a threshold around latitude 42° N. Our study align with this pattern, and suggest that the location of the latitudinal threshold dividing the Italian climate may have varied slightly through time and space.

During the early Holocene period (12,000–8,000 years cal. BP), the south of 43° N is characterised by relatively cold and wet summer conditions, regardless of elevation, while the north of 43° N is rather associated with hot and dry ones, particularly at high elevation (Fig. 5, A3), which is in line with the observations made by Magny et al. (2012) at this period. Winter conditions were however rather cold and dry throughout the early Holocene period (Fig. 6, A4), in contrast to what was suggested by the aforementioned study. The mid Holocene period (8,000–5,000 years cal. BP) was associated with relatively warm and humid winter conditions in the main part of Italy. Warmer and drier summers are reconstructed south of 43° N, in contrast to wetter summers recorded north of 43° N. This pattern for the mid Holocene differs from the Magny et al. (2013) study which reported humid winters/dry summers north of ca. 40° N and humid winters and summers south of 40° N during the mid Holocene. From the mid-to-late Holocene transition onward (5,000 years cal. BP to modern-day), winter and summer climate trends south of 43° N are globally similar to the mid Holocene ones while colder climate conditions following the HTM are depicted in summer from the sites located north of 43° N at high elevation (Fig. 5a).

In the Mediterranean, the seasonal and spatial variability of precipitation is directly linked to the global atmospheric circulation (Trigo and DaCamara, 2000). In their study, Magny et al. (2013) highlighted the combined effects of the blocking of the North Atlantic anticyclone linked to variations in summer insolation and the influence of ice sheets and the forcing of freshwater melt in the North Atlantic Ocean, both of which have an impact on large-scale circulation processes such as the NAO. In addition to global atmospheric circulation, other more local factors, such as orography, latitude and oceanic and continental influences, are directly linked to the seasonal and spatial variability of precipitation. The intricate topography of central Italy, combined with its central location within the Mediterranean basin, leads to precipitation patterns that arise from a variety of meteorological processes and influences, including flows from the south–west, west, north–east, and south–east (Silvestri et al., 2022). This complexity complicates the relationship between precipitation variability and alterations in large-scale atmospheric circulation, rendering the connections among precipitation fluxes, orography, and the spatial distribution of rainfall more intricate than in other regions characterised by simpler precipitation mechanisms (Silvestri et al., 2022), such as those predominantly influenced by westerly winds, as seen in Southern California (Millán et al., 2005; Hughes et al., 2009).

4.4 A west–east climate gradient in the central Mediterranean

The north-south climate contract does not appear to be the only specific climate dynamic in the Mediterranean basin. Roberts et al. (2011, 2012) have shown in a synthesis on the mid Holocene climate transition that both proxy data and model outputs suggested a west–east division in the Mediterranean climate history. Specifically, western Mediterranean early Holocene changes in precipitation were significantly smaller in magnitude and spatially less coherent than the eastern ones, and the mid

https://doi.org/10.5194/egusphere-2025-1106
Preprint. Discussion started: 14 March 2025

Holocene (around 6,000–3,000 years cal. BP) recorded the rainfall maximum before a decline to present-day values. Studies suggest that these contrasting hydroclimate regimes indicate a complicated interaction between different atmospheric systems, e.g., the main phases of NAO-like circulation (Fletcher et al., 2013; Di Rita et al., 2018), the East Atlantic pattern and the size and position of the North African anticyclone, that express differently in various sectors of the Mediterranean (Joannin et al., 2014b; Di Rita et al., 2018). This longitudinal component of the Mediterranean climate is also found in our study, which contrast the western regions of southern France with the northern Italian regions (Figs. 5b and 6b), and placing the central zone of southern France in a zone where the climatic signal is much more contrasted, suggesting the presence of a "buffer zone" where the different atmospheric dynamics confront each other. However, this hypothesis merits a more detailed regional study in order to understand the complexity of this transition zone, located in the southern part of the Massif Central region where relatively high elevation are encountered (> 600 m) and several climatic influences come together, i.e., Mediterranean influence from the south; the influence of the Atlantic Ocean from the west due to Atlantic air masses arriving from the country's west coast, which are not prevented by any geographical barriers obstacles in the Aquitaine Basin; and a mountainous regime from the north.

4.5 Spatio-temporal climate trends in the Mediterranean area during the Holocene

Our climate reconstruction, based on 38 records located in the central Mediterranean, highlights reliable spatio-temporal patterns at a regional scale despite an expected variability across the records that could reflect differences in latitude, elevation or in situ characteristics. We thus reconstruct homogeneous winter conditions in contrast to summers which were characterised by a marked north–south reversal throughout the Holocene (Fig. 5, 6).

4.5.1 Data–model comparison

Our results have been compared with the GCMs transient simulations TraCE-21ka (Collins et al., 2006). Comparison between data and model simulations will give us a better understanding of the climate mechanisms and their forcings. As the forcings implemented in TraCE-21ka are known (i.e., changes in orbital configuration and atmospheric greenhouse gases, the extent, topography and changing palaeogeography of ice sheets and scenario of freshwater forcing to the oceans from the retreating ice sheets), consistency or inconsistencies between the reconstructions and the simulations will enable us to highlight the forcings involved in the observed climate variations.

Pollen data and TraCE-21ka simulations show a winter warming throughout the Holocene (Fig. 8b-d). Discrepancies are evidenced in the precipitation estimates for the early Holocene period (pollen: dry conditions, TraCE-21ka: wet conditions) but models and data are in relatively good agreement for the mid-to-late Holocene (Fig. 7e). The range of anomaly values based on models (-19.5 to 24.8 mm $\pm$ 5.6 mm) is lower than the values derived from pollen data (-110.7 to 35.6 mm $\pm$ 20.3 mm). TraCE model simulations indicate a gradual summer humidification during the Holocene, although with a more accentuated humidification for regions north of 43° N than for those south of 43° N (Fig. 7d), which contrasts with the pollen-based summer aridification south of 43° N. The model simulations with TraCE-21ka (Fig. 7d, 8a) do not evidence the north–south latitudinal patterns depicted by the pollen climate reconstruction. Indeed, the simulated trends are consistent between the north of 43° N

https://doi.org/10.5194/egusphere-2025-1106
Preprint. Discussion started: 14 March 2025

and the south of 43° N, with colder summer conditions at the beginning of the Holocene, followed by a warming, a thermal maximum from 8,000 to 5,000 years cal. BP, then a gradual cooling. The thermal maximum during the mid Holocene period is more pronounced in regions located north of 43° N, such pattern is consistent with other model simulations for northern Europe and follows the change of summer insolation at those latitudes, which peaked at the onset of the Holocene (Mauri et al., 2015; Russo and Cubasch, 2016).

The data–model discrepancies may be explained by known biases in the spatial distribution of continental precipitation of the CCSM3 simulations (Collins et al., 2006) and by the coarse spatial resolution ($\geq 0.5°$) of GCMs as CCMS3 (Karger et al., 2023). Regional models will be more helpful to simulate the climate conditions during the Holocene at the Mediterranean scale (Brayshaw et al., 2011; Peyron et al., 2017) as they can reproduce realistic climatology with respect to the observations (Russo and Cubasch, 2016; Russo et al., 2022).

4.5.2 Winter: a warming trend in the Mediterranean region

Our pollen-inferred climate reconstruction indicates wet conditions on either side of 43° N in the central Mediterranean from 8,000 years cal. BP (Fig. 7b). The timing depends on the latitude: the wetter conditions are recorded around 7,500 years cal. BP at the north of 43° N, and 11,000 years cal. BP at the south of 43° N followed by a gradual increase until present-day values.

For temperatures, a rapid warming is reconstructed from 12,000 to 9,000 years cal. BP followed by a temperature increase throughout the Holocene, on either side of 43° N (Fig. 8d).

One of our goal was to study the climate changes in the central Mediterranean to fill the gap between the Iberian Peninsula (Fig. 8f) and Eastern Mediterranean (Fig. 8h) regions. Those two regions display the same winter warming trend through the Holocene despite having negative anomalies in contrast to our central Mediterranean winter temperature reconstructions. Winter warming associated with positive winter anomalies from 8,500 years BP onward are however present in the composite curves of Kaufman et al. (2020a) encompassing regions between the 30°–60° N parallels. This may suggest that the winter warming magnitude may vary regionally. The winter warming trend of the Mediterranean basin, induced by proxy data and model simulations, are similar and follows the variations in winter insolation for these latitudes, i.e., increasing trend, suggesting that insolation plays an important role and may be one of the main forcing of temperature variations in winter during the Holocene (Cruz-Silva et al., 2023; Liu et al., 2023).

https://doi.org/10.5194/egusphere-2025-1106
Preprint. Discussion started: 14 March 2025

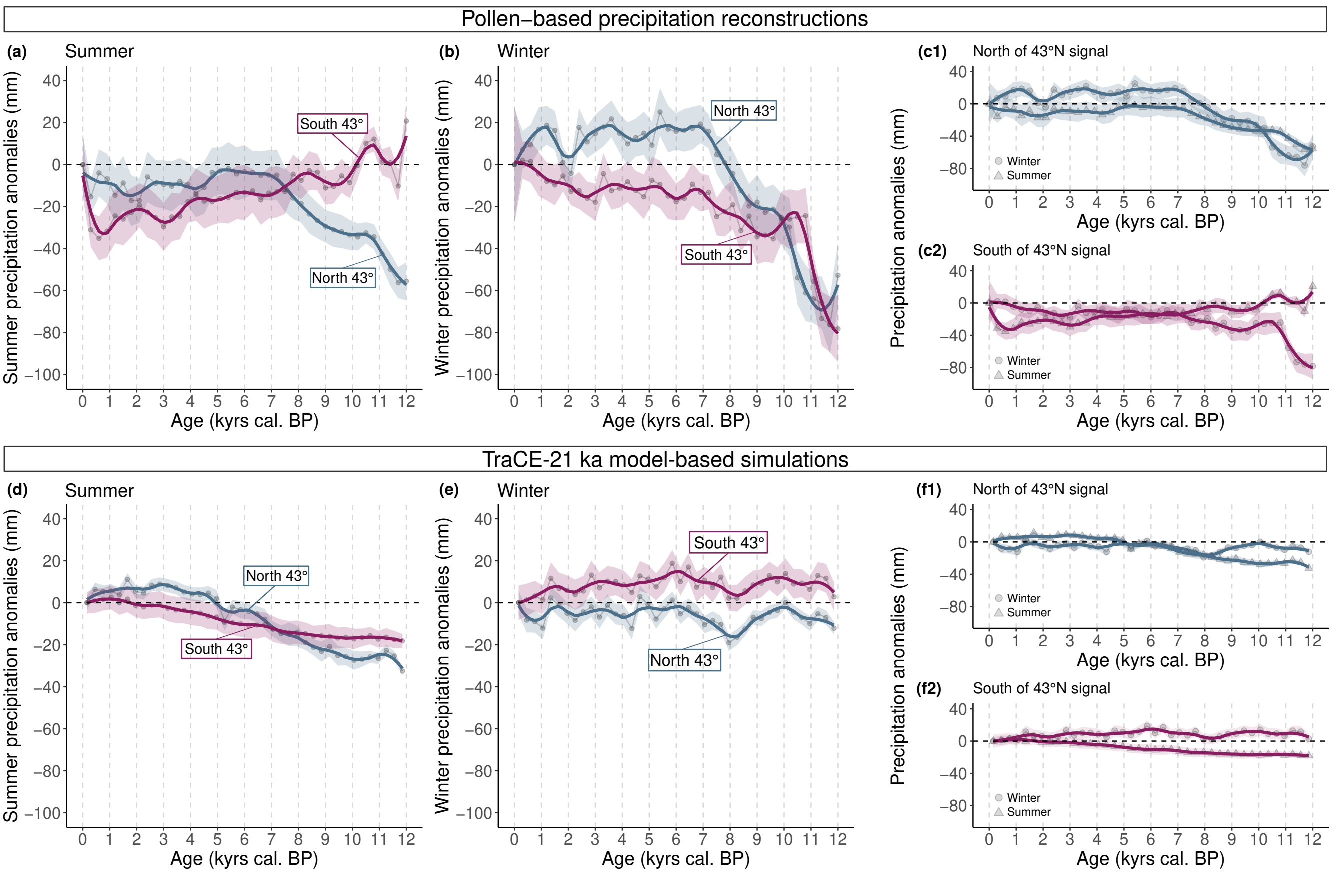

Figure 7. Reconstruction of the Holocene composite signal of the mean values across records for this study (north-central Mediterranean), using 300 years as the bin, expressed as anomalies relative to the current reconstructed values of respectively summer and winter precipitations (mm) from (a-b-c) the pollen-based signal and (d-e-f) the TraCE-21ka model-based signal. Total (convective and large-scale) precipitation rate (PRECT) was used to extract seasonal (summer and winter) precipitation simulations from the atmosphere post-processed data containing decadal mean seasonal averages. Output from the simulation was extracted for each pollen record location (Tab. 1). Composite curves were then constructed following the same process as pollen-based climate reconstruction. Shaded area corresponds to standard deviation values through a bootstrap resampling at the site level utilising 1000 iterations.

https://doi.org/10.5194/egusphere-2025-1106
Preprint. Discussion started: 14 March 2025

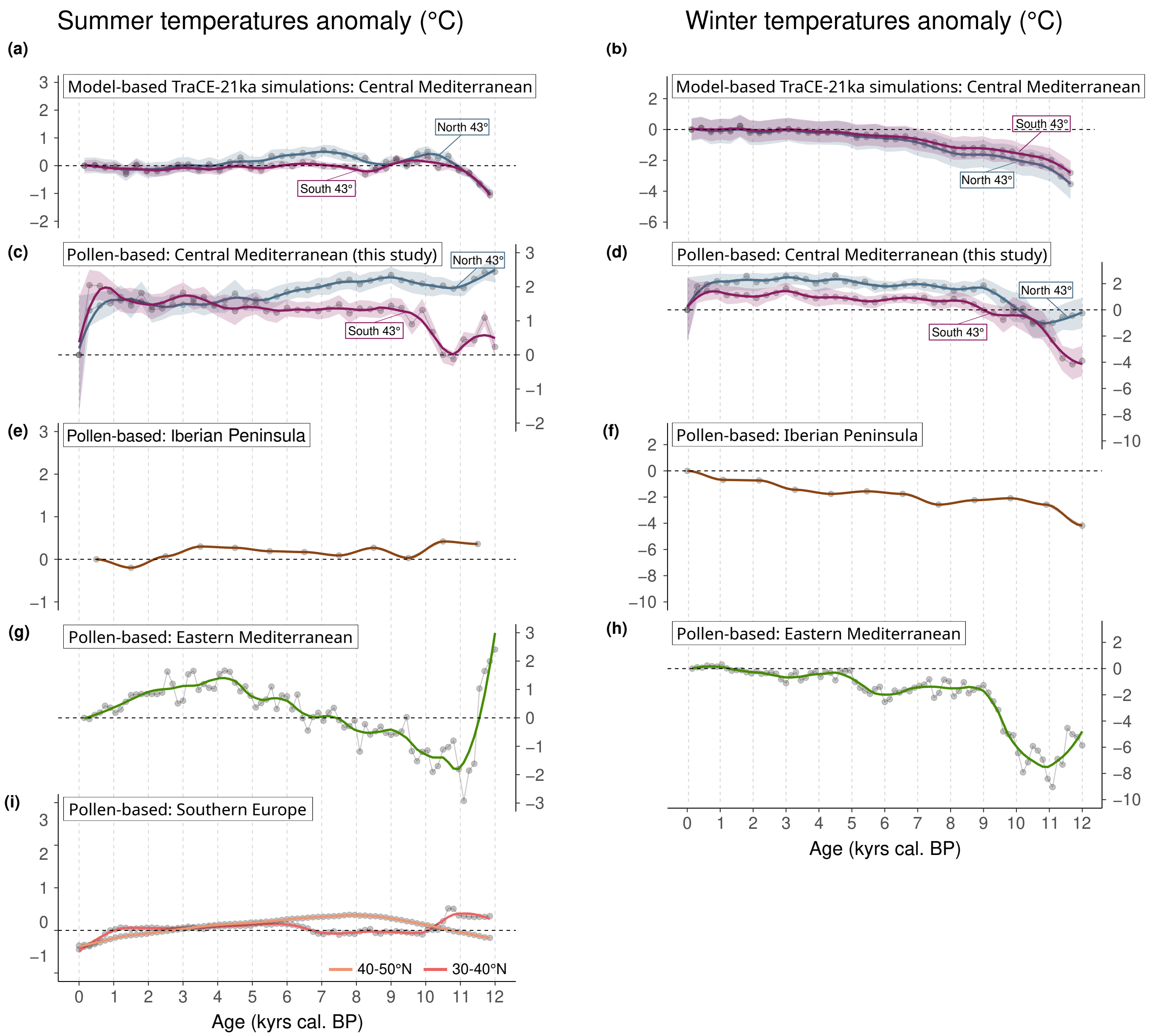

Figure 8. Reconstruction of the Holocene composite signal of the mean values across records for this study (north-central Mediterranean), using 300 years as the bin, expressed as anomalies relative to the current reconstructed values of respectively summer and winter temperatures (°C) from (a-b) the pollen-based signal and (c-d) the TraCE-21ka model-based signal. Surface temperature (TS) was used to extract seasonal (summer and winter) temperature simulations from the atmosphere post-processed data containing decadal mean seasonal averages. Output from the simulation was extracted for each pollen record location (Tab. 1). Composite curves were then constructed following the same process as pollen-based climate reconstruction. From (e) to (g), the reconstructed signal of summer temperatures for (e) the Iberian Peninsula (digitalised from Liu et al., 2023), (f) Eastern Mediterranean (Cruz-Silva et al., 2023) and (g) southern Europe (Herzschuh et al., 2023a). From (h) to (i), reconstructed signal of winter temperatures for (h) the Iberian Peninsula (digitalised from Liu et al., 2023), and (i) Eastern Mediterranean (Cruz-Silva et al., 2023). Shaded area corresponds to standard deviation values through a bootstrap resampling at the site level utilising 1000 iterations.

https://doi.org/10.5194/egusphere-2025-1106
Preprint. Discussion started: 14 March 2025

4.5.3 Summer: a contrasted spatio-temporal trend in the Mediterranean region

The summer trends are more contrasted than the winter ones and depend strongly on the latitude. While regions south of 43° N are characterised by a progressive decrease of summer precipitation throughout the Holocene, regions north of 43° N are characterised by dry conditions from 12,000 to 7,500 years cal. BP, followed by a mid Holocene wetness maximum (7,500–4,500 years cal. BP), before the gradual onset of summer aridification to present-day values (Fig. 7).

For the summer temperatures also, results seem strongly linked to the latitude. This is illustrated with the opposed climate trends north and south of 43° N (Fig. 8c). While the north of 43° N signal shows the presence of a summer thermal maximum (HTM) between 10,000–6,000 years cal. BP followed by a gradual cooling, regions located south of 43° N experienced a warming trend from 11,000 years cal. BP onward with warmer conditions during the late Holocene than during the mid Holocene (Fig. 8c). Similarly to our northern signal, the study of Zhang et al. (2022) highlighted an evident seasonal difference in southeastern Europe from pollen data, with a slightly warmer-than-present summer, associated with an early HTM between 10,000 and 8,000 years BP, but a cooler-than-present winter during the early Holocene before modern-day temperature are reached. Zhang et al. (2022) explained this seasonal difference by an orbital-induced seasonal insolation changes, playing a critical role in seasonal temperature evolutions, which in a long-term decrease in temperature seasonality during the Holocene.

This study provides new results on the well-debated question of whether southern Europe was colder than the north during the mid Holocene. Our results show that the mid Holocene was indeed colder than the late Holocene in the southern zone, but that the anomalies remain positive, while in the northern parts warmer conditions, associated with a HTM, were present. This should be nuanced, however, by the fact that the anomalies were calculated here in relation to the more recent reconstructed values (0–300 years binned) and not in relation to measured modern values, which could bias the anomaly calculation. Nevertheless, warmer or close to present-day summer temperature anomalies were present in the eastern, central and western Mediterranean (Fig. 8c-e-g-i) during the mid Holocene, questioning previous observations from pollen-based reconstructions showing colder temperatures in the Mediterranean region around 6,000 BP (Cheddadi et al., 1997; Davis et al., 2003; Mauri et al., 2015). Previous studies that depicted colder summer temperature in the Mediterranean around the mid Holocene used a similar pollen-based reconstruction method, i.e., Plant Fonctional Type (PFT) Modern Analogue Technique (MAT), while our study and the ones depicting a relatively close to modern-day summer temperature during the mid Holocene (Cruz-Silva et al., 2023; Herzschuh et al., 2023a; Liu et al., 2023) used different methods, i.e., a multi-method approach combining the MAT and BRT or a version of the Weigthed-Partial Least Squared (WA-PLS) method. This suggests that a method bias may be present, overestimating the cold values reconstructed in summer for the Mediterranean with the MAT method used by previous studies. The use of different methods producing similar results supports our observations and highlights the value of multi-method approaches for future studies based on pollen data to reconstruct palaeoclimates.

At a larger scale, we observe similar trends between the southern central Mediterranean (South 43° N) and the Eastern Mediterranean (Cruz-Silva et al., 2023, Fig. 8g), with warm conditions at the onset of the Holocene, followed by an abrupt cooling around 11,000 years cal. BP, and then by a gradual warming from 11,000 to 4,000 years cal. BP. This trend is not evidenced either on the Iberian peninsula or in the Herzschuh et al. (2023a) study (orange and coral lines respectively on Fig.

https://doi.org/10.5194/egusphere-2025-1106
Preprint. Discussion started: 14 March 2025

8g), focusing on Southern Europe (between latitudes 40–50° N and 30–40° N). On the other hand, even though the signal is slightly different, the Herzschuh et al. (2023a) study also clearly shows a different trend between the sites located north and south of 40° N, with a more pronounced optimum for the more northerly sites, which corroborates our results. In the Herzschuh et al. (2023a) study, some of the pollen records used to reconstruct the summer conditions for the 40–50° N area (orange line on Fig. 8i) are shared with our study, but a lot of their fossil records are located in the Alps, central and northern France, southern Germany and Bulgaria, regions with distinct climate dynamics compared to the Mediterranean ones, particularly in summer as the Mediterranean climate is known for its marked seasonality (Xoplaki et al., 2003). For the southern sites, few pollen records used in the Herzschuh et al. (2023a) study to reconstruct the 30–40° N climate signal (coral line on Fig. 8i) are shared with our study, and most of them are located in the southern Iberian Peninsula, in Greece and Anatolia. Modern-day climate dynamics are different in the western and eastern Mediterranean compared to the central region (Lionello et al., 2006), which may explain the differences observed between our reconstructions and the one proposed by Herzschuh et al. (2023a). This can explain some differences together with the method used, i.e., WA-PLS vs. combined MAT-BRT multi-method approach, and the modern pollen dataset used, i.e., global modern dataset encompassing 15,379 sites over Eurasia and North America vs. regional modern dataset.

However, other factors than methodology differences may explain the discrepancies obtained for the summer season. Indeed, the winter temperature signal reconstructed for the Iberian Peninsula, Eastern Mediterranean and the central Mediterranean is consistent between the studies, indicating that differences in methodology may not be the most important factor in explaining the summer climate trends observed. Another explanation could be the presence of a marked west–east Mediterranean climatic gradient (Roberts et al., 2011; Finné et al., 2019), probably present before the beginning of the Holocene, impacting the summer period and making the spatio-temporal pattern of summer climatic conditions much more complex than in winter.

4.5.4 Central Mediterranean seasonality evolution during the Holocene

The latitudinal component of the Mediterranean climate is also reflected in changes in precipitation seasonality. North of 43° N, summer and winter precipitation show similar increasing trends, although more pronounced in winter than in summer (Fig. 7c1). Regions south of 43° N show a different seasonal pattern, with increasingly arid summers and increasingly wet winters (Fig. 7c2). This phenomenon of "Mediterraneanization" of the Mediterranean basin took place during the mid Holocene after 8,000 years BP and seems to have had a greater impact on the southern regions than on the northern regions (Joannin et al., 2014a; Finné et al., 2019). The latitudinal variability of "Mediterraneanization" is also observed by Sadori et al. (2011), who showed that the expansion of drought-resistant taxa around the Mediterranean basin, which occurred principally after 8,000 years BP and was associated with a re-organisation of regional climate, was more pronounced in the southern regions of the central Mediterranean (e.g., Spain, Sicily, Croatia and southern Greece) than in central and northern Italy and the inner parts of the Balkans.

https://doi.org/10.5194/egusphere-2025-1106
Preprint. Discussion started: 14 March 2025

5 Conclusions

We aimed to document the climate changes of the central Mediterranean during the Holocene, the trends and the different patterns. A robust methodology has been applied to 38 pollen records spreading across the south of France and Italy. Four climate reconstruction methods based on different mathematical and ecological concepts have been tested (MAT, WA-PLS, BRT and RF) and the selection of the best modern calibration dataset has also been investigated to produce the most reliable results. Particular attention has been paid to the seasonal nature of climatic parameters (winter and summer temperatures and precipitations). A data-model comparison has been made using transient model simulation TraCE-21ka in an attempt to gain a better understanding of the climate mechanisms and their forcing.

Our palaeoclimate reconstruction shows that (1) during the mid Holocene, summer temperatures were colder in the southern part of the central Mediterranean region albeit associated with positive anomalies. This is in accordance with the summer temperature reconstructions of the Iberian peninsula, eastern Mediterranean and at a more regional scale of Southern Europe between 30° N to 50° N for the mid Holocene, showing anomalies close to modern-day values between 8,000 and 6,000 years BP. In northern parts of the central Mediterranean region, and particularly in high elevation ($\geq$ 1000 m), a Holocene thermal maximum is present. Those observations contrast with the cold summer temperature anomalies previously reconstructed with pollen data for the Mediterranean region. We suggest that a method bias may be responsible for an overestimation of cold summer temperature, highlighting the benefit of multi-method approaches, that could reduce the biases expressed by the use of a single method.

(2) Holocene summer conditions were characterised by specific spatio-temporal patterns, i.e., a west–east differentiation in southern France and a north–south one in Italy, for both temperature and precipitation. This latitudinal division on either side of 43° N for summer conditions confirms the initial hypotheses exposed by Magny et al. (2012, 2013) and Peyron et al. (2017), which correlated it with the decline of the possible blocking effects of the North Atlantic anticyclone linked to maximum insolation and of the influence of the remnant ice sheets and freshwater forcing in the North Atlantic ocean. Holocene winter conditions showed a more homogeneous spatio-temporal pattern, i.e., general humidification and warming through the Holocene for Italy and southern France. This spatial homogeneity of the winter climate through the Holocene is coherent with other pollen-based studies focusing on the Eastern Mediterranean and the Iberian Peninsula. Both a longitudinal, latitudinal and altitudinal dynamic define the spatio-temporal summer variability. Winter conditions in the north Mediterranean are much less affected by spatial characteristics and follow the increase in winter insolation at those latitudes. The presence of an west–east patterns, opposing the climate of western southern France and the north of Italy, support previous observations opposing the north-western and the south-eastern Mediterranean, highlighting the presence of complicated interaction between different atmospheric systems.

(3) Our pollen-based reconstructions with the TraCE-21ka transient simulations are mostly incoherent, particularly for precipitations, which may be explained by the presence of systematic biases in the spatial distribution of continental precipitation of CCSM3 simulations and from a still too coarse spatial resolution. The complex orography of the region with the presence of the Alps, the Pyrenees and the Apennines combined with the too-coarse spatial resolution of global climate models (GCMs)

https://doi.org/10.5194/egusphere-2025-1106
Preprint. Discussion started: 14 March 2025

prevent a good simulation of the spatial distribution of precipitation. Those discrepancies between model simulations and pollen-based reconstructions also suggest that during the Holocene, the northern Mediterranean climate was already subject to a marked spatio-temporal variability, particularly in summer, that cannot only be explained by changes in orbital configuration and atmospheric greenhouse gas evolution.

(4) Our result highlighted the onset of the "Mediterraneanization" of the central Mediterranean region, characterised by wet winters and dry summers, after 8,000 years BP. The "Mediterraneanization" process seems to have had a greater impact on the southern regions than on the northern regions.

This study has enabled us to further complete our understanding of the spatio-temporal variability of the north-central Mediterranean, in particular by comparing reconstructions based on similar methods applied to a corpus of pollen records. However, the limitations of this proxy are well known, although difficult to control and quantify, and the differences between reconstructions based on independent proxies have been highlighted on several occasions. This is why multi-proxy approaches, applied to several records, would make it possible to strengthen the robustness of our palaeoclimatic reconstructions based on pollen data. Several independent proxies have already been used in previous studies, such as chironomids for summer temperatures, oxygen isotopes for precipitation, and lipid biomarkers (e.g., alkenones and brGDGTs) for temperatures and environmental indicators. However, these studies remain relatively poor in the Mediterranean, highlighting the need to carry out these multi-proxy approaches on new sequences.

https://doi.org/10.5194/egusphere-2025-1106
Preprint. Discussion started: 14 March 2025

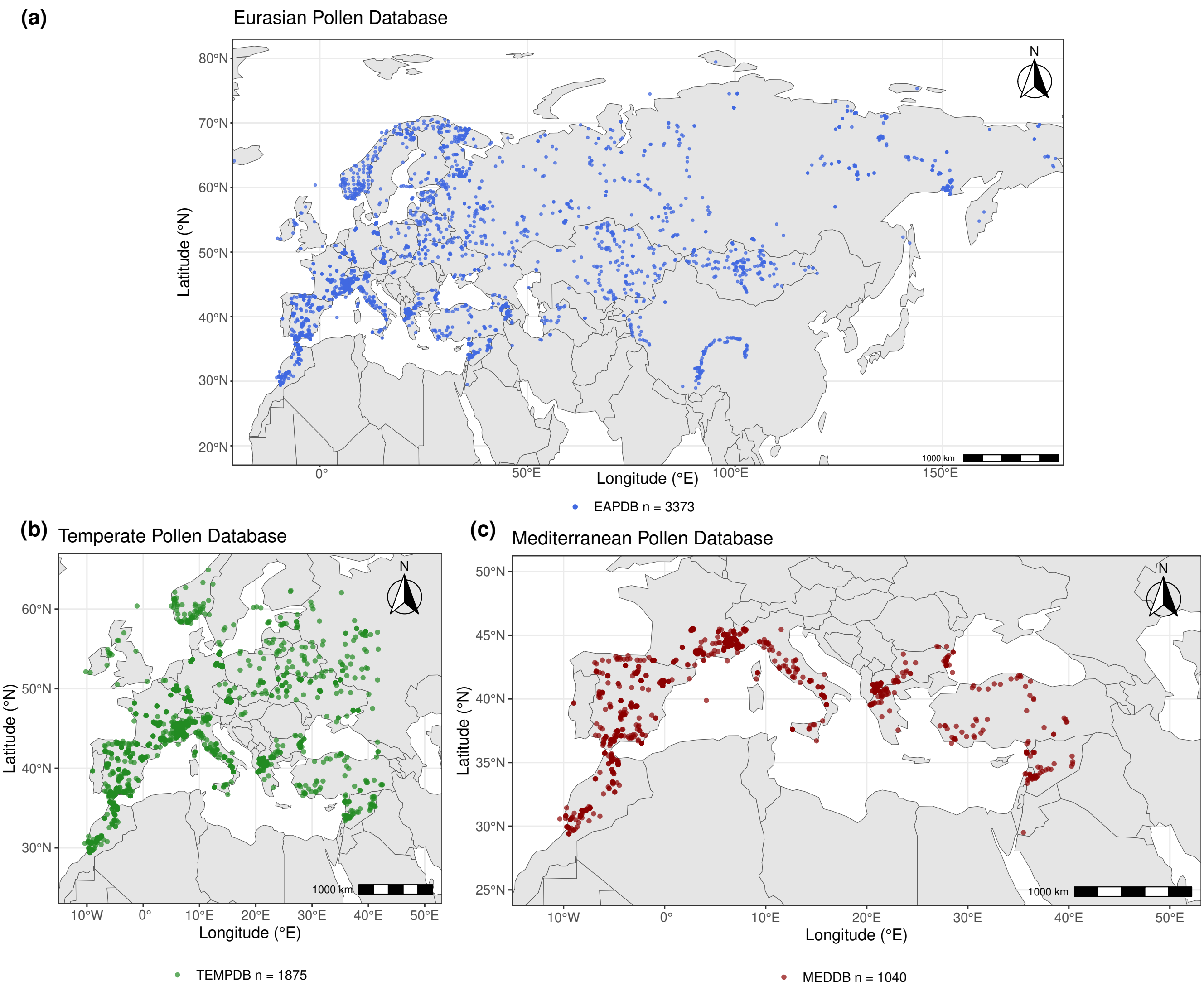

Figure A1. Location of surface sites used in (a) the Eurasian Pollen Dataset (EAPDB) compiled by (Peyron et al., 2013, 2017), (b) the Temperate Dataset (TEMPDB) and (c) the Mediterranean Dataset (MEDDB).

https://doi.org/10.5194/egusphere-2025-1106
Preprint. Discussion started: 14 March 2025

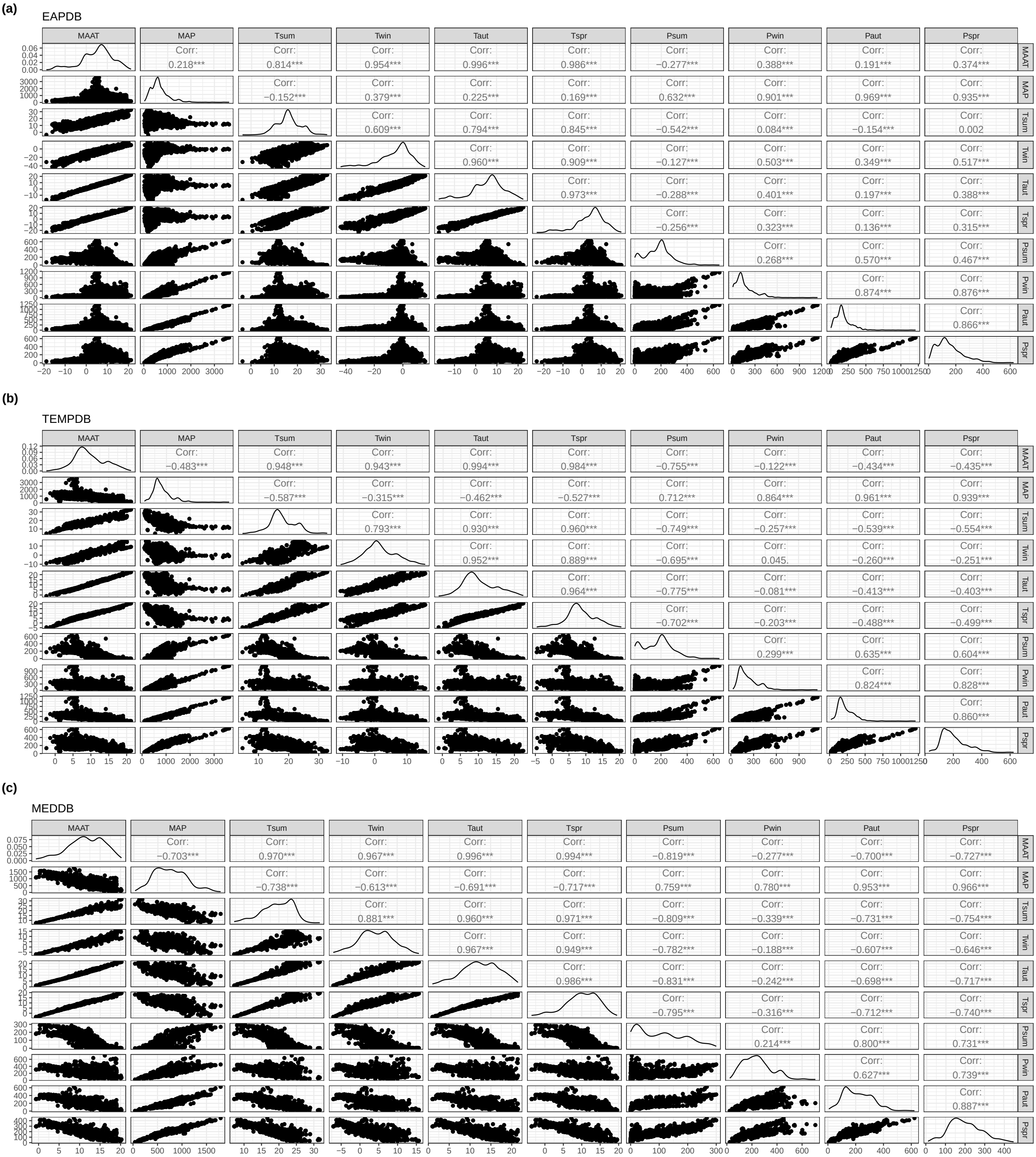

Figure A2. Pair-plots of the ten climatic variables (MAAT, MAP, Tsum, Twin Taut, Tspr, Psum, Pwin, Paut and Pspr) for (a) the Eurasian Pollen Dataset (EAPDB), (b) the Temperate Dataset (TEMPDB) and (c) the Mediterranean Dataset (MEDDB).

https://doi.org/10.5194/egusphere-2025-1106
Preprint. Discussion started: 14 March 2025

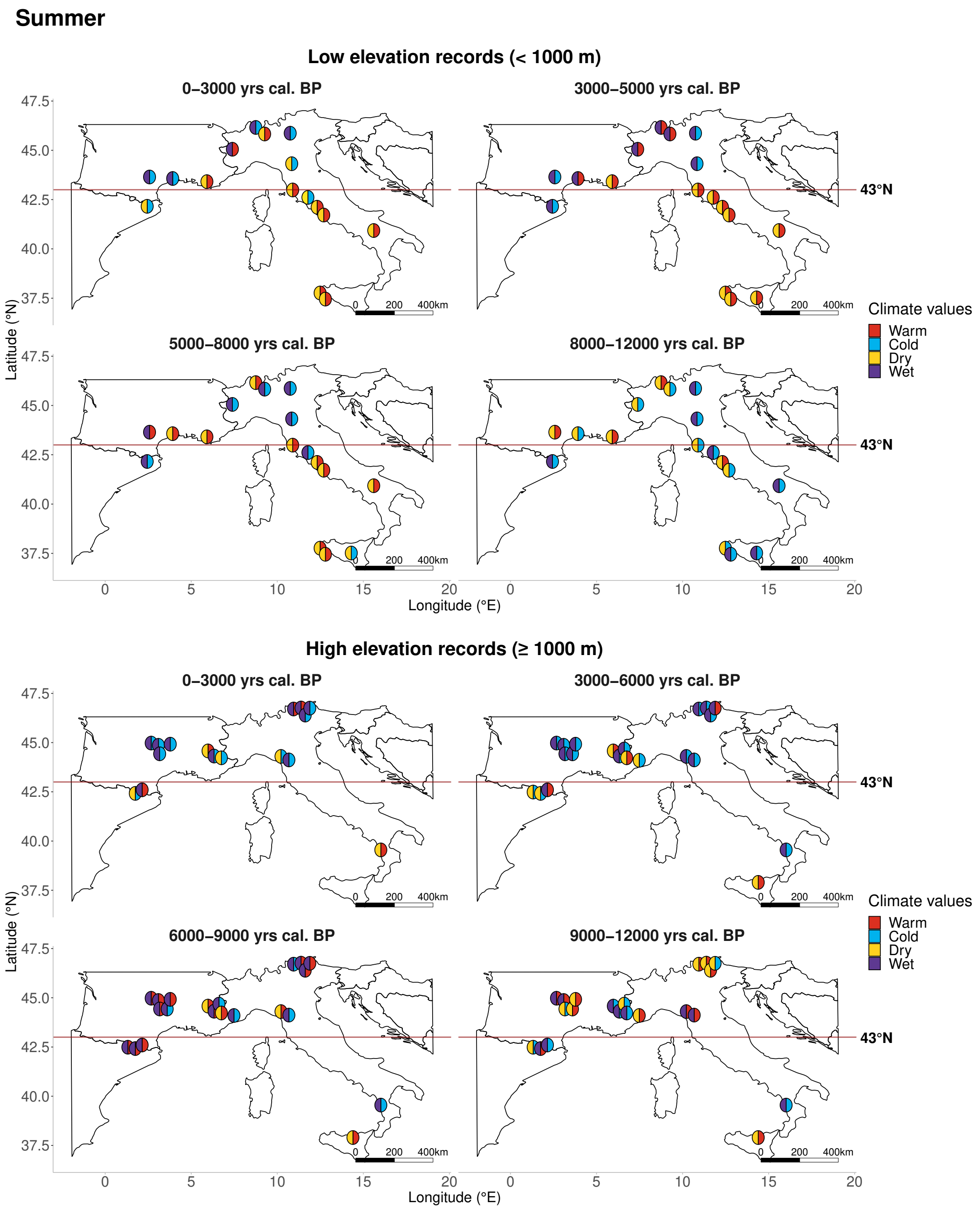

Figure A3. Maps of Holocene precipitation and temperature changes during the four designed periods of this study for summer conditions, where each record is represented by a disc divided into two parts with the precipitation information on one side (purple or yellow) and the temperature one on the other side (red or blue). The climate signal has been averaged through each period to propose an average trend for the period under consideration. The horizontal red line corresponds to the 43° N latitudinal delimitation characteristic of the north–south division of the Holocene Mediterranean climate.

https://doi.org/10.5194/egusphere-2025-1106
Preprint. Discussion started: 14 March 2025

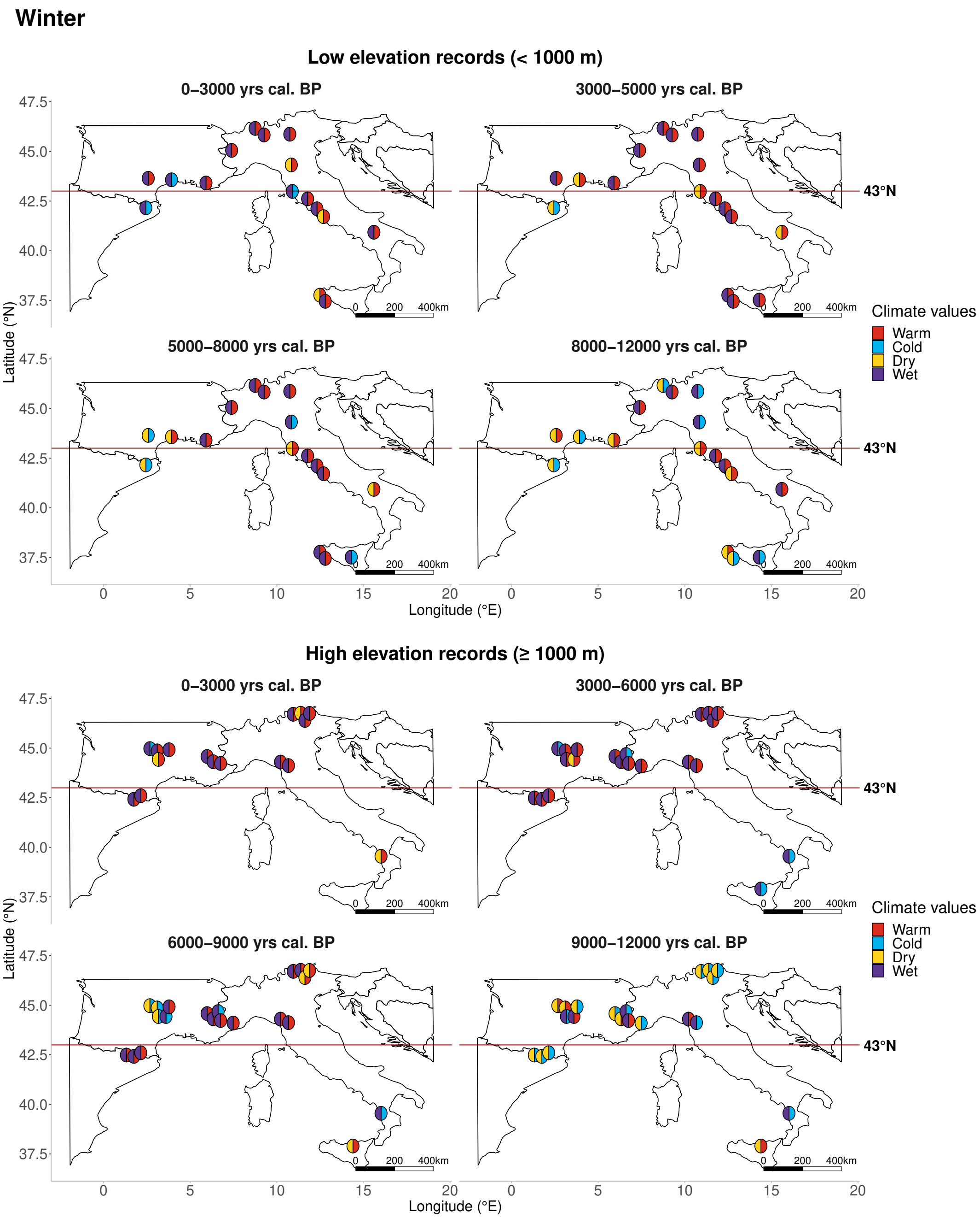

Figure A4. Maps of Holocene precipitation and temperature changes during the four designed periods of this study for winter conditions, where each record is represented by a disc divided into two parts with the precipitation information on one side (purple or yellow) and the temperature one on the other side (red or blue). The climate signal has been averaged through each period to propose an average trend for the period under consideration. The horizontal red line corresponds to the 43° N latitudinal delimitation characteristic of the north–south division of the Holocene Mediterranean climate.

https://doi.org/10.5194/egusphere-2025-1106
Preprint. Discussion started: 14 March 2025

Table A1. Variance inflation factors (VIFs) statistics including ten climate parameters for each of the modern datasets. VIF values < 10 are highlighted in bold. Ticks correspond to the absence of the climate parameter in the multicollinearity calculation.

	MAAT	MAP	**Tsum**	**Twin**	Taut	Tspr	**Psum**	**Pwin**	Paut	Pspr
EAPDB	544965.62	127.00	15063.97	78116.43	36146.23	34022.81	18.11	36.44	24.24	-
	-	126.99	21.57	80.50	135.19	46.42	18.08	36.40	24.22	-
	-	-	21.57	80.50	135.19	46.42	5.09	9.35	9.76	7.52
	-	-	14.42	21.67	-	43.0 9	4.91	9.33	9.52	7.29
	-	-	2.60	2.86	-	-	3.22	9.24	9.03	7.10
	-	-	**2.56**	**2.45**	-	-	**1.68**	**1.60**	-	-
TEMPDB	170519.23	157.66	10379.25	13520.43	11691.39	10409.15	30.71	38.89	23.67	-
	-	157.64	49.64	48.33	107.88	60.95	30.69	38.88	23.62	-
	-	-	49.64	48.33	107.88	60.95	8.91	7.78	8.66	7.46
	-	-	29.74	18.55	-	60.78	8.64	7.24	8.27	7.45
	-	-	4.39	3.95	-	-	4.46	6.85	7.07	6.50
	-	-	**3.87**	**3.73**	-	-	**2.76**	**1.45**	-	-
MEDDB	184683.87	192.85	11657.98	12169.64	11859.77	12569.80	30.29	48.19	31.48	-
	-	192.27	35.99	36.59	112.87	76.50	30.29	48.16	31.28	-
	-	-	35.99	36.59	112.87	76.50	9.66	7.06	9.03	11.69
	-	-	27.53	20.32	-	65.92	9.66	5.69	8.62	11.05
	-	-	5.96	4.87	-	-	8.19	5.65	7.66	11.02
	-	-	**5.80**	**4.59**	-	-	**3.12**	**1.21**	-	-

https://doi.org/10.5194/egusphere-2025-1106
Preprint. Discussion started: 14 March 2025

Data availability. A part of pollen data used are public access and accessible on the Neotoma Paleoecology Database (http://www.neotomadb.org). Access to data retrieved directly from the authors of the original studies should be requested directly from the authors. Palaeoclimate reconstruction will be fully available on PANGAEA.

Author contributions. Ld'O performed the analytical work, and LD designed the R codes; Ld'O, SJ, NC-N, MB, and OP designed the study; SJ, GM, NC-N, and OP supervised the study; AF, AM, AMM and LS provided part of the study material (fossil pollen sequences); LD, MB and MR contributed to data analysis; MB provided financial support for the project; Ld'O wrote the manuscript draft; SJ, GM, NC-N, LD, MB, MR, AF, AM, AMM, LS, MB and OP reviewed and edited the manuscript.

Competing interests. At least one of the (co-)authors (O. Peyron) is a member of the editorial board of Climate of the Past but the authors declare that they have no known competing financial interests or personal relationships that could have appeared to influence the work reported in this paper.

Acknowledgements. This study was financially supported by the ANR AUTUMN-LAMBS project (PI: M. Balasse). Data were obtained from the Neotoma Paleoecology Database (http://www.neotomadb.org) and its constituent database(s) see Table 1. Conference funding was provided by the Association des Palynologues de Langue Française (APLF). The work of data contributors, data stewards, and the Neotoma community is gratefully acknowledged. This is ISEM contribution XXXX-XXX.

https://doi.org/10.5194/egusphere-2025-1106
Preprint. Discussion started: 14 March 2025

References

Allen, J. R. M. and Huntley, B.: Effects of tephra falls on vegetation: A Late-Quaternary record from southern Italy, J Ecol, 106, 2456–2472, https://doi.org/10.1111/1365-2745.12998, 2018.

Azuara, J., Sabatier, P., Lebreton, V., Jalali, B., Sicre, M.-A., Dezileau, L., Bassetti, M.-A., Frigola, J., and Combourieu-Nebout, N.: Mid- to Late-Holocene Mediterranean climate variability: Contribution of multi-proxy and multi-sequence comparison using wavelet spectral analysis in the northwestern Mediterranean basin, Earth-Science Reviews, 208, 103 232, https://doi.org/10.1016/j.earscirev.2020.103232, 2020.

Bartlein, P. J., Harrison, S. P., Brewer, S., Connor, S., Davis, B. A. S., Gajewski, K., Guiot, J., Harrison-Prentice, T. I., Henderson, A., Peyron, O., Prentice, I. C., Scholze, M., Seppä, H., Shuman, B., Sugita, S., Thompson, R. S., Viau, A. E., Williams, J., and Wu, H.: Pollen-based continental climate reconstructions at 6 and 21 ka: a global synthesis, Clim Dyn, 37, 775–802, https://doi.org/10.1007/s00382-010-0904-1, 2011.

Beaulieu, J.-L. d. and Reille, M.: Paléoenvironnement tardiglaciaire et holocène des lacs de Pelléautier et Siguret (Hautes-Alpes, France). I. Histoire de la végétation d'après les analyses polliniques, Ecologia mediterranea, 9, 19–36, 1983.

Beniston, M., Diaz, H. F., and Bradley, R. S.: Climatic Change at High Elevation Sites: An Overview, in: Climatic Change at High Elevation Sites, edited by Diaz, H. F., Beniston, M., and Bradley, R. S., pp. 1–19, Springer Netherlands, https://doi.org/10.1007/978-94-015-8905-5_1, 1997.

Bini, M., Zanchetta, G., Perşoiu, A., Cartier, R., Català, A., Cacho, I., Dean, J. R., Di Rita, F., Drysdale, R. N., Finnè, M., Isola, I., Jalali, B., Lirer, F., Magri, D., Masi, A., Marks, L., Mercuri, A. M., Peyron, O., Sadori, L., Sicre, M.-A., Welc, F., Zielhofer, C., and Brisset, E.: The 4.2 ka BP Event in the Mediterranean region: an overview, Clim. Past, 15, 555–577, https://doi.org/10.5194/cp-15-555-2019, 2019.

Birks, H. J. B., Heiri, O., Seppä, H., and Bjune, A. E.: Strengths and Weaknesses of Quantitative Climate Reconstructions Based on Late-Quaternary Biological Proxies, The Open Ecology Journal, 3, 68–110, 2010.

Bisculm, M., Colombaroli, D., Vescovi, E., van Leeuwen, J. F. N., Henne, P. D., Rothen, J., Procacci, G., Pasta, S., La Mantia, T., and Tinner, W.: Holocene vegetation and fire dynamics in the supra-mediterranean belt of the Nebrodi Mountains (Sicily, Italy): HOLOCENE VEGETATION AND FIRE DYNAMICS IN SICILY, J. Quaternary Sci., 27, 687–698, https://doi.org/10.1002/jqs.2551, 2012.

Blaauw, M. and Christen, J. A.: Flexible paleoclimate age-depth models using an autoregressive gamma process, Bayesian Analysis, 6, 457 – 474, https://doi.org/10.1214/11-BA618, 2011.

Brandimarte, L., Di Baldassarre, G., Bruni, G., D'Odorico, P., and Montanari, A.: Relation Between the North-Atlantic Oscillation and Hydroclimatic Conditions in Mediterranean Areas, Water Resources Management, 25, 1269–1279, https://doi.org/10.1007/s11269-010-9742-5, 2011.

Brayshaw, D. J., Rambeau, C. M., and Smith, S. J.: Changes in Mediterranean climate during the Holocene: Insights from global and regional climate modelling, The Holocene, 21, 15–31, https://doi.org/10.1177/0959683610377528, 2011.

Breiman, L.: Random Forests, Machine Learning, 45, 5–32, https://doi.org/10.1023/A:1010933404324, 2001.

Brewer, S., Guiot, J., Sánchez-Goñi, M., and Klotz, S.: The climate in Europe during the Eemian: a multi-method approach using pollen data, Quaternary Science Reviews, 27, 2303–2315, https://doi.org/10.1016/j.quascirev.2008.08.029, 2008.

Calò, C., Henne, P. D., Curry, B., Magny, M., Vescovi, E., La Mantia, T., Pasta, S., Vannière, B., and Tinner, W.: Spatio-temporal patterns of Holocene environmental change in southern Sicily, Palaeogeography, Palaeoclimatology, Palaeoecology, 323-325, 110–122, https://doi.org/10.1016/j.palaeo.2012.01.038, 2012.

Cao, X.-y., Herzschuh, U., Telford, R. J., and Ni, J.: A modern pollen–climate dataset from China and Mongolia: Assessing its potential for climate reconstruction, Review of Palaeobotany and Palynology, 211, 87–96, https://doi.org/10.1016/j.revpalbo.2014.08.007, 2014.

Cartapanis, O., Jonkers, L., Moffa-Sanchez, P., Jaccard, S. L., and de Vernal, A.: Complex spatio-temporal structure of the Holocene Thermal Maximum, Nat Commun, 13, 5662, https://doi.org/10.1038/s41467-022-33362-1, 2022.

Cheddadi, R., Yu, G., Guiot, J., Harrison, S. P., and Prentice, I. C.: The climate of Europe 6000 years ago, Climate Dynamics, 13, 1–9, 1997.

Chevalier, M., Davis, B., Heiri, O., Seppä, H., Chase, B. M., Gajewski, K., Lacourse, T., Telford, R. J., Finsinger, W., Guiot, J., Kühl, N., Maezumi, S. Y., Tipton, J. R., Carter, V. A., Brussel, T., Phelps, L. N., Dawson, A., Zanon, M., Vallé, F., Nolan, C., Mauri, A., de Vernal, A., Izumi, K., Holmström, L., Marsicek, J., Goring, S., Sommer, P. S., Chaput, M., and Kupriyanov, D.: Pollen-based climate reconstruction techniques for late Quaternary studies, Earth-Science Reviews, 210, 33, 2020.

Collins, W. D., Bitz, C. M., Blackmon, M. L., Bonan, G. B., Bretherton, C. S., Carton, J. A., Chang, P., Doney, S. C., Hack, J. J., Henderson, T. B., Kiehl, J. T., Large, W. G., McKenna, D. S., Santer, B. D., and Smith, R. D.: The Community Climate System Model Version 3 (CCSM3), Journal of Climate, 19, 2122–2143, https://doi.org/10.1175/JCLI3761.1, 2006.

Cramer, W., Guiot, J., Fader, M., Garrabou, J., Gattuso, J.-P., Iglesias, A., Lange, M. A., Lionello, P., Llasat, M. C., Paz, S., Peñuelas, J., Snoussi, M., Toreti, A., Tsimplis, M. N., and Xoplaki, E.: Climate change and interconnected risks to sustainable development in the Mediterranean, Nature Climate Change, 8, 972–980, https://doi.org/10.1038/s41558-018-0299-2, 2018.

Cruz-Silva, E., Harrison, S. P., Prentice, I. C., Marinova, E., Bartlein, P. J., Renssen, H., and Zhang, Y.: Pollen-based reconstructions of Holocene climate trends in the eastern Mediterranean region, Clim. Past, 19, 2093–2108, https://doi.org/10.5194/cp-19-2093-2023, 2023.

Davis, B., Brewer, S., Stevenson, A., and Guiot, J.: The temperature of Europe during the Holocene reconstructed from pollen data, Quaternary Science Reviews, 22, 1701–1716, https://doi.org/10.1016/S0277-3791(03)00173-2, 2003.

De Beaulieu, J. and Jorda, M.: Tardiglaciaire et Postglaciaire des Alpes de Haute-Provence. Le glaciaire de la Blanche, Trois évêchés, quate, 14, 3–15, https://doi.org/10.3406/quate.1977.1307, 1977.

De Beaulieu, J., Pons, A., and Reille, M.: Recherches pollenanalytiques sur l'histoire tardiglaciaire et holocene de la vegetation des Monts d'Aubrac (Massif Central, France), Review of Palaeobotany and Palynology, 44, 37–80, https://doi.org/10.1016/0034-6667(85)90028-4, 1985.

de Beaulieu, J.-L.: Evolution de la végétation sur la bordure montagneuse cévenole au postglaciaire, d'après les pollens, 1974.

De Beaulieu, J.-L., Miras, Y., Andrieu-Ponel, V., and Guiter, F.: Vegetation dynamics in north-western Mediterranean regions: Instability of the Mediterranean bioclimate, 139, 114–126, https://doi.org/10.1080/11263500500197858, 2005.

Di Bernardino, A., Iannarelli, A. M., Casadio, S., and Siani, A. M.: Winter warm spells over Italy: Spatial–temporal variation and large-scale atmospheric circulation, International Journal of Climatology, 44, 1262–1275, https://doi.org/10.1002/joc.8388, 2024.

Di Rita, F., Fletcher, W. J., Aranbarri, J., Margaritelli, G., Lirer, F., and Magri, D.: Holocene forest dynamics in central and western Mediterranean: periodicity, spatio-temporal patterns and climate influence, Sci Rep, 8, 8929, https://doi.org/10.1038/s41598-018-27056-2, 2018.

d'Oliveira, L., Dugerdil, L., Ménot, G., Evin, A., Muller, S. D., Ansanay-Alex, S., Azuara, J., Bonnet, C., Bremond, L., Shah, M., and Peyron, O.: Reconstructing 15 000 years of southern France temperatures from coupled pollen and molecular (branched glycerol dialkyl glycerol tetraether) markers (Canroute, Massif Central), Climate of the Past, 19, 2127–2156, https://doi.org/10.5194/cp-19-2127-2023, 2023.

Dormoy, I., Peyron, O., Nebout, N. C., Goring, S., Kotthoff, U., Magny, M., and Pross, J.: Terrestrial climate variability and seasonality changes in the Mediterranean region between 15 000 and 4000 years BP deduced from marine pollen records, Clim. Past, 2009.

Drescher-Schneider, R., de Beaulieu, J.-L., Magny, M., Walter-Simonnet, A.-V., Bossuet, G., Millet, L., Brugiapaglia, E., and Drescher, A.: Vegetation history, climate and human impact over the last 15,000 years at Lago dell'Accesa (Tuscany, Central Italy), Veget Hist Archaeobot, 16, 279–299, https://doi.org/10.1007/s00334-006-0089-z, 2007.

Dugerdil, L., Joannin, S., Peyron, O., Jouffroy-Bapicot, I., Vannière, B., Boldgiv, B., Unkelbach, J., Behling, H., and Ménot, G.: Climate reconstructions based on GDGT and pollen surface datasets from Mongolia and Baikal area: calibrations and applicability to extremely cold–dry environments over the Late Holocene, Clim. Past, 17, 1199–1226, https://doi.org/10.5194/cp-17-1199-2021, 2021a.

Dugerdil, L., Ménot, G., Peyron, O., Jouffroy-Bapicot, I., Ansanay-Alex, S., Antheaume, I., Behling, H., Boldgiv, B., Develle, A.-L., Grossi, V., Magail, J., Makou, M., Robles, M., Unkelbach, J., Vannière, B., and Joannin, S.: Late Holocene Mongolian climate and environment reconstructions from brGDGTs, NPPs and pollen transfer functions for Lake Ayrag: Paleoclimate implications for Arid Central Asia, Quaternary Science Reviews, 273, 107 235, https://doi.org/10.1016/j.quascirev.2021.107235, 2021b.

Erb, M. P., McKay, N. P., Steiger, N., Dee, S., Hancock, C., Ivanovic, R. F., Gregoire, L. J., and Valdes, P.: Reconstructing Holocene temperatures in time and space using paleoclimate data assimilation, Clim. Past, 18, 2599–2629, https://doi.org/10.5194/cp-18-2599-2022, 2022.

Fick, S. E. and Hijmans, R. J.: WorldClim 2: new 1-km spatial resolution climate surfaces for global land areas, International Journal of Climatology, 37, 4302–4315, https://doi.org/10.1002/joc.5086, 2017.

Finné, M., Woodbridge, J., Labuhn, I., and Roberts, C. N.: Holocene hydro-climatic variability in the Mediterranean: A synthetic multi-proxy reconstruction, The Holocene, 29, 847–863, https://doi.org/10.1177/0959683619826634, 2019.

Finsinger, W. and Tinner, W.: Holocene vegetation and land-use changes in response to climatic changes in the forelands of the southwestern Alps, Italy, J. Quaternary Sci., 21, 243–258, https://doi.org/10.1002/jqs.971, 2006.

Finsinger, W., Lane, C. S., van Den Brand, G. J., Wagner-Cremer, F., Blockley, S., and Lotter, A.: The Lateglacial Quercus expansion in the southern European Alps: rapid vegetation response to a late Allerød climate warming?, Journal of Quaternary Science, 26, 694–702, 2011.

Finsinger, W., Vanel, Q., Ribolini, A., and Tinner, W.: Early to late Holocene vegetation and fire dynamics at the treeline in the Maritime Alps, Veget Hist Archaeobot, 30, 507–524, https://doi.org/10.1007/s00334-020-00795-x, 2021.

Fletcher, W. J., Debret, M., and Goñi, M. F. S.: Mid-Holocene emergence of a low-frequency millennial oscillation in western Mediterranean climate: Implications for past dynamics of the North Atlantic atmospheric westerlies, The Holocene, 23, 153–166, https://doi.org/10.1177/0959683612460783, 2013.

Fratianni, S. and Acquaotta, F.: The Climate of Italy, in: Landscapes and Landforms of Italy, edited by Soldati, M. and Marchetti, M., pp. 29–38, Springer International Publishing, https://doi.org/10.1007/978-3-319-26194-2_4, series Title: World Geomorphological Landscapes, 2017.

Giraudi, C., Magny, M., Zanchetta, G., and Drysdale, R.: The Holocene climatic evolution of Mediterranean Italy: A review of the continental geological data, The Holocene, 21, 105–115, https://doi.org/10.1177/0959683610377529, 2011.

Gobet, E., Tinner, W., Hubschmid, P., Jansen, I., Wehrli, M., Ammann, B., and Wick, L.: Influence of human impact and bedrock differences on the vegetational history of the Insubrian Southern Alps, Veget Hist Archaebot, 9, 175–187, https://doi.org/10.1007/BF01299802, 2000.

Goudeau, M.-L. S., Reichart, G.-J., Wit, J., De Nooijer, L., Grauel, A.-L., Bernasconi, S., and De Lange, G.: Seasonality variations in the Central Mediterranean during climate change events in the Late Holocene, Palaeogeography, Palaeoclimatology, Palaeoecology, 418, 304–318, https://doi.org/10.1016/j.palaeo.2014.11.004, 2015.

Guiot, J.: Methodology of the last climatic cycle reconstruction in France from pollen data, Palaeogeography, Palaeoclimatology, Palaeoecology, 80, 49–69, https://doi.org/10.1016/0031-0182(90)90033-4, 1990.

https://doi.org/10.5194/egusphere-2025-1106
Preprint. Discussion started: 14 March 2025

Guiter, F., Andrieu-Ponel, V., Digerfeldt, G., Reille, M., de Beaulieu, J.-L., and Ponel, P.: Vegetation history and lake-level changes from the Younger Dryas to the present in Eastern Pyrenees (France): pollen, plant macrofossils and lithostratigraphy from Lake Racou (2000 m a.s.l.), Veget Hist Archaeobot, 14, 99–118, https://doi.org/10.1007/s00334-005-0065-z, 2005.

Herzschuh, U., Li, C., Böhmer, T., Postl, A. K., Heim, B., Andreev, A. A., Cao, X., Wieczorek, M., and Ni, J.: LegacyPollen 1.0: a taxonomically harmonized global late Quaternary pollen dataset of 2831 records with standardized chronologies, Earth Syst. Sci. Data, 14, 3213–3227, https://doi.org/10.5194/essd-14-3213-2022, 2022.

Herzschuh, U., Böhmer, T., Chevalier, M., Hébert, R., Dallmeyer, A., Li, C., Cao, X., Peyron, O., Nazarova, L., Novenko, E. Y., Park, J., Rudaya, N. A., Schlütz, F., Shumilovskikh, L. S., Tarasov, P. E., Wang, Y., Wen, R., Xu, Q., and Zheng, Z.: Regional pollen-based Holocene temperature and precipitation patterns depart from the Northern Hemisphere mean trends, Clim. Past, 19, 1481–1506, https://doi.org/10.5194/cp-19-1481-2023, 2023a.

Herzschuh, U., Böhmer, T., Li, C., Chevalier, M., Hébert, R., Dallmeyer, A., Cao, X., Bigelow, N. H., Nazarova, L., Novenko, E. Y., Park, J., Peyron, O., Rudaya, N. A., Schlütz, F., Shumilovskikh, L. S., Tarasov, P. E., Wang, Y., Wen, R., Xu, Q., and Zheng, Z.: LegacyClimate 1.0: a dataset of pollen-based climate reconstructions from 2594 Northern Hemisphere sites covering the last 30 kyr and beyond, Earth System Science Data, 15, 2235–2258, https://doi.org/10.5194/essd-15-2235-2023, 2023b.

Hijmans, R. J., Phillips, S., Leathwick, J., and Elith, J.: dismo: Species Distribution Modeling, CRAN, https://rspatial.org/raster/sdm/, r package version 1.3-16, 2024.

Hill, M. O. and Gauch, H. G.: Detrended Correspondence Analysis: An Improved Ordination Technique, in: Classification and Ordination: Symposium on advances in vegetation science, Nijmegen, The Netherlands, May 1979, edited by van der Maarel, E., pp. 47–58, Springer Netherlands, Dordrecht, https://doi.org/10.1007/978-94-009-9197-2_7, 1980.

Hofstetter, S., Tinner, W., Valsecchi, V., Carraro, G., and Conedera, M.: Lateglacial and Holocene vegetation history in the Insubrian Southern Alps—new indications from a small-scale site, Vegetation history and archaeobotany, 15, 87–98, 2006.

Hughes, M., Hall, A., and Fovell, R. G.: Blocking in Areas of Complex Topography, and Its Influence on Rainfall Distribution, Journal of the Atmospheric Sciences, 66, 508–518, https://doi.org/10.1175/2008JAS2689.1, 2009.

Jalut, G.: Changements climatiques holocènes en Méditerranée occidentale: mise en place du climat méditerranéen, Pallas, pp. 13–34, 2000.

Jalut, G., Esteban Amat, A., Bonnet, L., Gauquelin, T., and Fontugne, M.: Holocene climatic changes in the Western Mediterranean, from south-east France to south-east Spain, Palaeogeography, Palaeoclimatology, Palaeoecology, 160, 255–290, https://doi.org/10.1016/S0031-0182(00)00075-4, 2000.

Joannin, S., Brugiapaglia, E., de Beaulieu, J.-L., Bernardo, L., Magny, M., Peyron, O., Goring, S., and Vannière, B.: Pollen-based reconstruction of Holocene vegetation and climate in southern Italy: the case of Lago Trifoglietti, Clim. Past, 8, 1973–1996, https://doi.org/10.5194/cp-8-1973-2012, 2012.

Joannin, S., Vannière, B., Galop, D., Peyron, O., Haas, J. N., Gilli, A., Chapron, E., Wirth, S. B., Anselmetti, F., Desmet, M., and Magny, M.: Climate and vegetation changes during the Lateglacial and early–middle Holocene at Lake Ledro (southern Alps, Italy), Clim. Past, 9, 913–933, https://doi.org/10.5194/cp-9-913-2013, 2013.

Joannin, S., Ali, A. A., Ollivier, V., Roiron, P., Peyron, O., Chevaux, S., Nahapetyan, S., Tozalakyan, P., Karakhanyan, A., and Chataigner, C.: Vegetation, fire and climate history of the Lesser Caucasus: a new Holocene record from Zarishat fen (Armenia), Journal of Quaternary Science, 29, 70–82, https://doi.org/10.1002/jqs.2679, publisher: Wiley, 2014a.

Joannin, S., Magny, M., Peyron, O., Vannière, B., and Galop, D.: Climate and land-use change during the late Holocene at Lake Ledro (southern Alps, Italy), The Holocene, 24, 591–602, https://doi.org/10.1177/0959683614522311, 2014b.

https://doi.org/10.5194/egusphere-2025-1106
Preprint. Discussion started: 14 March 2025

Juggins, S.: rioja: Analysis of Quaternary Science Data, CRAN, https://cran.r-project.org/package=rioja, r package version 1.0-7, 2024.

Karger, D. N., Nobis, M. P., Normand, S., Graham, C. H., and Zimmermann, N. E.: CHELSA-TraCE21k – high-resolution (1 km) downscaled transient temperature and precipitation data since the Last Glacial Maximum, Climate of the Past, 19, 439–456, https://doi.org/10.5194/cp-19-439-2023, 2023.

Kaufman, D., McKay, N., Routson, C., Erb, M., Davis, B., Heiri, O., Jaccard, S., Tierney, J., Dätwyler, C., Axford, Y., Brussel, T., Cartapanis, O., Chase, B., Dawson, A., de Vernal, A., Engels, S., Jonkers, L., Marsicek, J., Moffa-Sánchez, P., Morrill, C., Orsi, A., Rehfeld, K., Saunders, K., Sommer, P. S., Thomas, E., Tonello, M., Tóth, M., Vachula, R., Andreev, A., Bertrand, S., Biskaborn, B., Bringué, M., Brooks, S., Caniupán, M., Chevalier, M., Cwynar, L., Emile-Geay, J., Fegyveresi, J., Feurdean, A., Finsinger, W., Fortin, M.-C., Foster, L., Fox, M., Gajewski, K., Grosjean, M., Hausmann, S., Heinrichs, M., Holmes, N., Ilyashuk, B., Ilyashuk, E., Juggins, S., Khider, D., Koinig, K., Langdon, P., Larocque-Tobler, I., Li, J., Lotter, A., Luoto, T., Mackay, A., Magyari, E., Malevich, S., Mark, B., Massaferro, J., Montade, V., Nazarova, L., Novenko, E., Pařil, P., Pearson, E., Peros, M., Pienitz, R., Płóciennik, M., Porinchu, D., Potito, A., Rees, A., Reinemann, S., Roberts, S., Rolland, N., Salonen, S., Self, A., Seppä, H., Shala, S., St-Jacques, J.-M., Stenni, B., Syrykh, L., Tarrats, P., Taylor, K., van den Bos, V., Velle, G., Wahl, E., Walker, I., Wilmshurst, J., Zhang, E., and Zhilich, S.: A global database of Holocene paleotemperature records, Sci Data, 7, 115, https://doi.org/10.1038/s41597-020-0445-3, 2020a.

Kaufman, D., McKay, N., Routson, C., Erb, M., Dätwyler, C., Sommer, P. S., Heiri, O., and Davis, B.: Holocene global mean surface temperature, a multi-method reconstruction approach, Sci Data, 7, 201, https://doi.org/10.1038/s41597-020-0530-7, 2020b.

Kelly, M. G. and Huntley, B.: An 11 000-year record of vegetation and environment from Lago di Martignano, Latium, Italy, J. Quaternary Sci., 6, 209–224, https://doi.org/10.1002/jqs.3390060304, 1991.

Li, C., Postl, A. K., Böhmer, T., Cao, X., Dolman, A. M., and Herzschuh, U.: Harmonized chronologies of a global late Quaternary pollen dataset (LegacyAge 1.0), Earth Syst. Sci. Data, 14, 1331–1343, https://doi.org/10.5194/essd-14-1331-2022, 2022.

Lionello, P., Malanotte-Rizzoli, P., Boscolo, R., Alpert, P., Artale, V., Li, L., Luterbacher, J., May, W., Trigo, R., Tsimplis, M., Ulbrich, U., and Xoplaki, E.: The Mediterranean climate: An overview of the main characteristics and issues, in: Mediterranean, edited by Lionello, P., Malanotte-Rizzoli, P., and Boscolo, R., vol. 4 of *Developments in Earth and Environmental Sciences*, pp. 1–26, Elsevier, https://doi.org/https://doi.org/10.1016/S1571-9197(06)80003-0, 2006.

Liu, M., Shen, Y., González-Sampériz, P., Gil-Romera, G., Ter Braak, C. J. F., Prentice, I. C., and Harrison, S. P.: Holocene climates of the Iberian Peninsula: pollen-based reconstructions of changes in the west–east gradient of temperature and moisture, Climate of the Past, 19, 803–834, https://doi.org/10.5194/cp-19-803-2023, 2023.

Liu, Z., Zhu, J., Rosenthal, Y., Zhang, X., Otto-Bliesner, B. L., Timmermann, A., Smith, R. S., Lohmann, G., Zheng, W., and Elison Timm, O.: The Holocene temperature conundrum, Proceedings of the National Academy of Sciences, 111, E3501–E3505, https://doi.org/10.1073/pnas.1407229111, 2014.

Magny, M., Bégeot, C., Guiot, J., and Peyron, O.: Contrasting patterns of hydrological changes in Europe in response to Holocene climate cooling phases, Quaternary Science Reviews, 22, 1589–1596, https://doi.org/10.1016/S0277-3791(03)00131-8, 2003.

Magny, M., Peyron, O., Sadori, L., Ortu, E., Zanchetta, G., Vannière, B., and Tinner, W.: Contrasting patterns of precipitation seasonality during the Holocene in the south- and north-central Mediterranean, J. Quaternary Sci., 27, 290–296, https://doi.org/10.1002/jqs.1543, 2012.

Magny, M., Combourieu-Nebout, N., de Beaulieu, J. L., Bout-Roumazeilles, V., Colombaroli, D., Desprat, S., Francke, A., Joannin, S., Ortu, E., Peyron, O., Revel, M., Sadori, L., Siani, G., Sicre, M. A., Samartin, S., Simonneau, A., Tinner, W., Vannière, B., Wagner, B., Zanchetta, G., Anselmetti, F., Brugiapaglia, E., Chapron, E., Debret, M., Desmet, M., Didier, J., Essallami, L., Galop, D., Gilli, A., Haas, J. N., Kallel, N., Millet, L., Stock, A., Turon, J. L., and Wirth, S.: North–south palaeohydrological contrasts in the central Mediterranean during the Holocene: tentative synthesis and working hypotheses, Clim. Past, 9, 2043–2071, https://doi.org/10.5194/cp-9-2043-2013, 2013.

Margaritelli, G., Cacho, I., Català, A., Barra, M., Bellucci, L. G., Lubritto, C., Rettori, R., and Lirer, F.: Persistent warm Mediterranean surface waters during the Roman period, Scientific Reports, 10, 10 431, https://doi.org/10.1038/s41598-020-67281-2, 2020.

Marignani, M., Chiarucci, A., Sadori, L., and Mercuri, A. M.: Natural and human impact in Mediterranean landscapes: An intriguing puzzle or only a question of time?, Plant Biosystems - An International Journal Dealing with all Aspects of Plant Biology, 151, 900–905, https://doi.org/10.1080/11263504.2016.1244121, 2017.

Marriner, N., Kaniewski, D., Pourkerman, M., and Devillers, B.: Anthropocene tipping point reverses long-term Holocene cooling of the Mediterranean Sea: A meta-analysis of the basin's Sea Surface Temperature records, Earth-Science Reviews, 227, 103 986, https://doi.org/10.1016/j.earscirev.2022.103986, 2022.

Marsicek, J., Shuman, B. N., Bartlein, P. J., Shafer, S. L., and Brewer, S.: Reconciling divergent trends and millennial variations in Holocene temperatures, Nature, 554, 92–96, https://doi.org/10.1038/nature25464, 2018.

Mauri, A., Davis, B. A. S., Collins, P. M., and Kaplan, J. O.: The influence of atmospheric circulation on the mid-Holocene climate of Europe: a data–model comparison, Clim. Past, 10, 1925–1938, https://doi.org/10.5194/cp-10-1925-2014, 2014.

Mauri, A., Davis, B., Collins, P., and Kaplan, J.: The climate of Europe during the Holocene: a gridded pollen-based reconstruction and its multi-proxy evaluation, Quaternary Science Reviews, 112, 109–127, https://doi.org/10.1016/j.quascirev.2015.01.013, 2015.

Mercuri, A. M., Accorsi, C. A., and Bandini Mazzanti, M.: The long history of Cannabis and its cultivation by the Romans in central Italy, shown by pollen records from Lago Albano and Lago di Nemi, Vegetation History and Archaeobotany, 11, 263–276, https://doi.org/10.1007/s003340200039, 2002.

Mercuri, A. M., Mazzanti, M. B., Florenzano, A., Montecchi, M. C., and Rattighieri, E.: Olea, Juglans and Castanea: the OJC group as pollen evidence of the development of human-induced environments in the Italian peninsula, Quaternary international, 303, 24–42, 2013.

Millán, M. M., Estrela, M. J., and Miró, J.: Rainfall Components: Variability and Spatial Distribution in a Mediterranean Area (Valencia Region), Journal of Climate, 18, 2682–2705, https://doi.org/10.1175/JCLI3426.1, 2005.

Miras, Y., Ejarque, A., Riera, S., Palet, J. M., Orengo, H., and Euba, I.: Dynamique holocène de la végétation et occupation des Pyrénées andorranes depuis le Néolithique ancien, d'après l'analyse pollinique de la tourbière de Bosc dels Estanyons (2180m, Vall del Madriu, Andorre), Comptes Rendus Palevol, 6, 291–300, https://doi.org/10.1016/j.crpv.2007.02.005, 2007.

Miras, Y., Ejarque, A., Orengo, H., Mora, S. R., Palet, J. M., and Poiraud, A.: Prehistoric impact on landscape and vegetation at high altitudes: An integrated palaeoecological and archaeological approach in the eastern Pyrenees (Perafita valley, Andorra), Plant Biosystems - An International Journal Dealing with all Aspects of Plant Biology, 144, 924–939, https://doi.org/10.1080/11263504.2010.491980, 2010.

Nakagawa, T.: Études palynologiques dans les Alpes françaises centrales et méridionales: histoire de la végétation tardiglaciaire et holocène, Ph.D. thesis, Aix-Marseille 3, 1998.

Nicol-Pichard, S.: Analyse pollinique d'une séquence tardi et postglaciaire à Tourves (Var, France), ecmed, 13, 29–42, https://doi.org/10.3406/ecmed.1987.1609, 1987.

Ortu, E., Brewer, S., and Peyron, O.: Pollen-inferred palaeoclimate reconstructions in mountain areas: problems and perspectives, J. Quaternary Sci., 21, 615–627, https://doi.org/10.1002/jqs.998, 2006.

Ortu, E., David, F., and Peyron, O.: Pollen-inferred palaeoclimate reconstruction in the Alps during the Lateglacial and the early Holocene: how to estimate the effect of elevation and local parameters, 25, 651–661, https://doi.org/10.1002/jqs.1335, 2010.

https://doi.org/10.5194/egusphere-2025-1106
Preprint. Discussion started: 14 March 2025

Peyron, O., Bégeot, C., Brewer, S., Heiri, O., Magny, M., Millet, L., Ruffaldi, P., Van Campo, E., and Yu, G.: Late-Glacial climatic changes in Eastern France (Lake Lautrey) from pollen, lake-levels, and chironomids, Quat. res., 64, 197–211, https://doi.org/10.1016/j.yqres.2005.01.006, 2005.

Peyron, O., Goring, S., Dormoy, I., Kotthoff, U., Pross, J., de Beaulieu, J.-L., Drescher-Schneider, R., Vannière, B., and Magny, M.: Holocene seasonality changes in the central Mediterranean region reconstructed from the pollen sequences of Lake Accesa (Italy) and Tenaghi Philippon (Greece), The Holocene, 21, 131–146, https://doi.org/10.1177/0959683610384162, 2011.

Peyron, O., Magny, M., Goring, S., Joannin, S., de Beaulieu, J.-L., Brugiapaglia, E., Sadori, L., Garfi, G., Kouli, K., Ioakim, C., and Combourieu-Nebout, N.: Contrasting patterns of climatic changes during the Holocene across the Italian Peninsula reconstructed from pollen data, Clim. Past, 9, 1233–1252, https://doi.org/10.5194/cp-9-1233-2013, 2013.

Peyron, O., Combourieu-Nebout, N., Brayshaw, D., Goring, S., Andrieu-Ponel, V., Desprat, S., Fletcher, W., Gambin, B., Ioakim, C., Joannin, S., Kotthoff, U., Kouli, K., Montade, V., Pross, J., Sadori, L., and Magny, M.: Precipitation changes in the Mediterranean basin during the Holocene from terrestrial and marine pollen records: a model–data comparison, Clim. Past, 13, 249–265, https://doi.org/10.5194/cp-13-249-2017, 2017.

Piqué, R., Revelles, J., Burjachs, F., Caruso Fermé, L., and Pérez-Obiol, R.: Interdisciplinary approach to the landscape and firewood exploitation during the Holocene at La Garrotxa (Girona, NE Iberia), Quaternary International, 463, 401–413, https://doi.org/10.1016/j.quaint.2016.11.025, 2018.

Prentice, I.: Multidimensional scaling as a research tool in quaternary palynology: A review of theory and methods, Review of Palaeobotany and Palynology, 31, 71–104, https://doi.org/10.1016/0034-6667(80)90023-8, 1980.

Puertas, O.: Évolution holocène de la végétation en bordure de l'étang de Méjean : analyse pollinique du sondage d'Embouchac (Lattes, Hérault, France)[Holocene vegetation dynamic on the edge of the Méjean lagune ; pollen analysis of Embouchac boring (Lattes, Hérault, France)], quate, 9, 79–89, https://doi.org/10.3406/quate.1998.1591, 1998.

Puertas, O.: Premiers indices polliniques de néolithisation dans la plaine littorale de Montpellier (Hérault, France), Bulletin de la Société préhistorique française, pp. 15–20, 1999.

Pérez-Obiol, R.: Histoire tardiglaciaire et holocène de la végétation de la région volcanique d'Olot (NE Péninsule Ibérique), Pollen et spores, 30, 189–202, 1988.

Reille, M. and De Beaulieu, J.: History of the Würm and Holocene vegetation in western Velay (Massif Central, France): a comparison of pollen analysis from three corings at Lac du Bouchet, Review of Palaeobotany and Palynology, 54, 233–248, 1988.

Reimer, P. J., Austin, W. E. N., Bard, E., Bayliss, A., Blackwell, P. G., Bronk Ramsey, C., Butzin, M., Cheng, H., Edwards, R. L., Friedrich, M., Grootes, P. M., Guilderson, T. P., Hajdas, I., Heaton, T. J., Hogg, A. G., Hughen, K. A., Kromer, B., Manning, S. W., Muscheler, R., Palmer, J. G., Pearson, C., van der Plicht, J., Reimer, R. W., Richards, D. A., Scott, E. M., Southon, J. R., Turney, C. S. M., Wacker, L., Adolphi, F., Büntgen, U., Capano, M., Fahrni, S. M., Fogtmann-Schulz, A., Friedrich, R., Köhler, P., Kudsk, S., Miyake, F., Olsen, J., Reinig, F., Sakamoto, M., Sookdeo, A., and Talamo, S.: The IntCal20 Northern Hemisphere Radiocarbon Age Calibration Curve (0–55 cal kBP), Radiocarbon, 62, 725–757, https://doi.org/10.1017/RDC.2020.41, 2020.

Renssen, H., Seppä, H., Crosta, X., Goosse, H., and Roche, D.: Global characterization of the Holocene Thermal Maximum, Quaternary Science Reviews, 48, 7–19, https://doi.org/10.1016/j.quascirev.2012.05.022, 2012.

Revelles, J., Burjachs, F., Palomo, A., Piqué, R., Iriarte, E., Pérez-Obiol, R., and Terradas, X.: Human-environment interaction during the Mesolithic- Neolithic transition in the NE Iberian Peninsula. Vegetation history, climate change and human impact during the Early-Middle Holocene in the Eastern Pre-Pyrenees, Quaternary Science Reviews, 184, 183–200, https://doi.org/10.1016/j.quascirev.2017.08.025, 2018.

Roberts, N., Brayshaw, D., Kuzucuoğlu, C., Perez, R., and Sadori, L.: The mid-Holocene climatic transition in the Mediterranean: Causes and consequences, The Holocene, 21, 3–13, https://doi.org/10.1177/0959683610388058, 2011.

Roberts, N., Moreno, A., Valero-Garcés, B. L., Corella, J. P., Jones, M., Allcock, S., Woodbridge, J., Morellón, M., Luterbacher, J., Xoplaki, E., and Türkeş, M.: Palaeolimnological evidence for an east–west climate see-saw in the Mediterranean since AD 900, Global and Planetary Change, 84-85, 23–34, https://doi.org/10.1016/j.gloplacha.2011.11.002, 2012.

Robles, M., Peyron, O., Brugiapaglia, E., Ménot, G., Dugerdil, L., Ollivier, V., Ansanay-Alex, S., Develle, A.-L., Tozalakyan, P., Meliksetian, K., Sahakyan, K., Sahakyan, L., Perello, B., Badalyan, R., Colombié, C., and Joannin, S.: Impact of climate changes on vegetation and human societies during the Holocene in the South Caucasus (Vanevan, Armenia): A multiproxy approach including pollen, NPPs and brGDGTs, Quaternary Science Reviews, 277, 107 297, https://doi.org/10.1016/j.quascirev.2021.107297, 2022.

Robles, M., Peyron, O., Ménot, G., Brugiapaglia, E., Wulf, S., Appelt, O., Blache, M., Vannière, B., Dugerdil, L., Paura, B., Ansanay-Alex, S., Cromartie, A., Charlet, L., Guédron, S., De Beaulieu, J.-L., and Joannin, S.: Climate changes during the Late Glacial in southern Europe: new insights based on pollen and brGDGTs of Lake Matese in Italy, Clim. Past, 19, 493–515, https://doi.org/10.5194/cp-19-493-2023, 2023.

Russo, E. and Cubasch, U.: Mid-to-late Holocene temperature evolution and atmospheric dynamics over Europe in regional model simulations, Climate of the Past, 12, 1645–1662, https://doi.org/10.5194/cp-12-1645-2016, 2016.

Russo, E., Fallah, B., Ludwig, P., Karremann, M., and Raible, C. C.: The long-standing dilemma of European summer temperatures at the mid-Holocene and other considerations on learning from the past for the future using a regional climate model, Climate of the Past, 18, 895–909, https://doi.org/10.5194/cp-18-895-2022, 2022.

Sadori, L.: The Lateglacial and Holocene vegetation and climate history of Lago di Mezzano (central Italy), Quaternary Science Reviews, 202, 30–44, https://doi.org/10.1016/j.quascirev.2018.09.004, 2018.

Sadori, L. and Narcisi, B.: The Postglacial record of environmental history from Lago di Pergusa, Sicily, The Holocene, 11, 655–671, https://doi.org/10.1191/09596830195681, 2001.

Sadori, L., Jahns, S., and Peyron, O.: Mid-Holocene vegetation history of the central Mediterranean, The Holocene, 21, 117–129, https://doi.org/10.1177/0959683610377530, 2011.

Salonen, J. S., Korpela, M., Williams, J. W., and Luoto, M.: Machine-learning based reconstructions of primary and secondary climate variables from North American and European fossil pollen data, Sci Rep, 9, 15 805, https://doi.org/10.1038/s41598-019-52293-4, 2019.

Samartin, S., Heiri, O., Joos, F., Renssen, H., Franke, J., Brönnimann, S., and Tinner, W.: Warm Mediterranean mid-Holocene summers inferred from fossil midge assemblages, Nature Geosci, 10, 207–212, https://doi.org/10.1038/ngeo2891, 2017.

Sassoon, D., Combourieu-Nebout, N., Peyron, O., Bertini, A., Toti, F., Lebreton, V., and Moncel, M.-H.: Pollen-based climatic reconstructions for the interglacial analogues of MIS 1 (MIS 19, 11, and 5) in the southwestern Mediterranean: insights from ODP Site 976, Climate of the Past, 21, 489–515, https://doi.org/10.5194/cp-21-489-2025, 2025.

Seiwald, A.: Beiträge zur Vegetationsgeschichte Tirols. 4. Natzer Plateau-Villanderer Alm, Universitätsverlag Wagner, Innsbruck, Österreich, 1979.

Silvestri, L., Saraceni, M., and Bongioannini Cerlini, P.: Links between precipitation, circulation weather types and orography in central Italy, International Journal of Climatology, 42, 5807–5825, https://doi.org/10.1002/joc.7563, 2022.

Sugita, S.: A Model of Pollen Source Area for an Entire Lake Surface, Quaternary Research, 39, 239–244, https://doi.org/10.1006/qres.1993.1027, 1993.

Surmely, F., Miras, Y., Guenet, P., Nicolas, V., Savignat, A., Vannière, B., Walter-Simonnet, A.-V., Servera, G., and Tzortzis, S.: Occupation and land-use history of a medium mountain from the Mid-Holocene: A multidisciplinary study performed in the South Cantal (French Massif Central), Comptes Rendus Palevol, 8, 737–748, https://doi.org/10.1016/j.crpv.2009.07.002, 2009.

Team, R.: RStudio: Integrated Development Environment for R, RStudio, PBC., Boston, MA, http://www.rstudio.com/, 2020.

Ter Braak, C. J. and Prentice, I.: A Theory of Gradient Analysis, in: Advances in Ecological Research, vol. 34, pp. 235–282, Elsevier, https://doi.org/10.1016/S0065-2504(03)34003-6, 1988.

ter Braak, C. J. F. and Juggins, S.: Weighted averaging partial least squares regression (WA-PLS): an improved method for reconstructing environmental variables from species assemblages | SpringerLink, Hydrobiologia, 269/270, 485–502, https://link.springer.com/article/10.1007/BF00028046, 1993.

Ter Braak, C. J. F. and Verdonschot, P. F. M.: Canonical correspondence analysis and related multivariate methods in aquatic ecology, Aquatic Science, 57, 255–289, https://doi.org/10.1007/BF00877430, 1995.

Thouveny, N., Creer, K., and Blunk, I.: Extension of the Lac du Bouchet palaeomagnetic record over the last 120,000 years, Earth and Planetary Science Letters, 97, 140–161, https://doi.org/10.1016/0012-821X(90)90105-7, 1990.

Tinner, W., van Leeuwen, J. F., Colombaroli, D., Vescovi, E., van der Knaap, W. O., Henne, P. D., Pasta, S., D'Angelo, S., and La Mantia, T.: Holocene environmental and climatic changes at Gorgo Basso, a coastal lake in southern Sicily, Italy, Quaternary Science Reviews, 28, 1498–1510, 2009.

Trasune, L., Väliranta, M., Stivrins, N., Amon, L., Schenk, F., and Salonen, J. S.: A comparison of plant macrofossil-based quantitative climate reconstruction methods: A case study of the lateglacial Baltic States, Quaternary Science Reviews, 338, 108 811, https://doi.org/10.1016/j.quascirev.2024.108811, 2024.

Trigo, R. M. and DaCamara, C. C.: Circulation weather types and their influence on the precipitation regime in Portugal, International Journal of Climatology, 20, 1559–1581, https://doi.org/10.1002/1097-0088(20001115)20:13<1559::AID-JOC555>3.0.CO;2-5, 2000.

Turner, M. G., Wei, D., Prentice, I. C., and Harrison, S. P.: The impact of methodological decisions on climate reconstructions using WA-PLS, Quaternary Research, 99, 341–356, https://doi.org/10.1017/qua.2020.44, publisher: Cambridge University Press, 2021.

Vescovi, E., Ammann, B., Ravazzi, C., and Tinner, W.: A new Late-glacial and Holocene record of vegetation and fire history from Lago del Greppo, northern Apennines, Italy, Veget Hist Archaeobot, 19, 219–233, https://doi.org/10.1007/s00334-010-0243-5, 2010a.

Vescovi, E., Kaltenrieder, P., and Tinner, W.: Late-Glacial and Holocene vegetation history of Pavullo nel Frignano (Northern Apennines, Italy), Review of Palaeobotany and Palynology, 160, 32–45, https://doi.org/10.1016/j.revpalbo.2010.01.002, 2010b.

Watson, C. S.: The vegetational history of the northern Apennines, Italy: information from three new sequences and a review of Regional vegetational change, J Biogeography, 23, 805–841, https://doi.org/10.1111/j.1365-2699.1996.tb00041.x, 1996.

Wickham, H.: ggplot2: Elegant Graphics for Data Analysis, Use R!, Springer International Publishing, Cham, https://doi.org/10.1007/978-3-319-24277-4, 2016.

Williams, J., Grimm, E., Blois, J., Charles, D., Davis, E., Goring, S., Graham, R., Smith, A., Anderson, M., Arroyo-Cabrales, J., Ashworth, A., Betancourt, J., Bills, B., Booth, R., Buckland, P., Curry, B., Giesecke, T., Hausmann, S., Jackson, S., Latorre, C., Nichols, J., Purdum, T., Roth, R., Stryker, M., and Takahara, H.: The Neotoma Paleoecology Database: A multi-proxy, international community-curated data resource, Quaternary Research, 89, 156–177, 2018.

Winschall, A., Sodemann, H., Pfahl, S., and Wernli, H.: How important is intensified evaporation for Mediterranean precipitation extremes?, Journal of Geophysical Research: Atmospheres, 119, 5240–5256, https://doi.org/10.1002/2013JD021175, 2014.

Xoplaki, E., González-Rouco, J. F., Luterbacher, J., and Wanner, H.: Mediterranean summer air temperature variability and its connection to the large-scale atmospheric circulation and SSTs, Climate Dynamics, 20, 723–739, https://doi.org/10.1007/s00382-003-0304-x, 2003.

Zhang, W., Wu, H., Cheng, J., Geng, J., Li, Q., Sun, Y., Yu, Y., Lu, H., and Guo, Z.: Holocene seasonal temperature evolution and spatial variability over the Northern Hemisphere landmass, Nature Communications, 13, 5334, https://doi.org/10.1038/s41467-022-33107-0, 2022.